GEOLOGICA CARPATHICA, 2026, 77, 5, 345–369 https://doi.org/10.31577/GeolCarp.2026.17

Scales of confinement in Lake Pannon turbidites, case studies from South Transdanubia, Hungary

LILLA TŐKÉS[1,✉] and ORSOLYA SZTANÓ[1]

[1]Department of Geology, ELTE Eötvös Loránd University, Budapest, Hungary

(Manuscript received May 12, 2026; accepted in revised form July 1, 2026; Associate Editor: Michal Šujan)

Abstract: Scales are fundamental in geology; the hierarchical architecture of deep-water turbidite systems, which controls hydrocarbon reservoir quality, is a prime example. The bottom topography confines turbidity currents by altering their route and influencing their deposition. Effects of confinement can be captured on different scales from the event scale, i.e. the bed scale, the architectural elements, and the turbidite systems up to basin scale. Exploring the relationship between basin geometries, sizes, and their effect on confinement can provide crucial insights into sedimentary dynamics. The Pannonian Basin had a highly irregular topography during both syn-rift and post-rift evolution, hosting the well-studied Lake Pannon sedimentary system, offering an ideal study area for confined turbidites. Published 2D seismic sections, net-to-gross and depth maps were used to analyse the basin-scale confinement in the Zala area, South Transdanubia, SW Pannonian Basin. Flattening and spectral decomposition on 3D seismic data from the Mezőcsokonya and Drava basins was done as part of paleotopographical and geomorphological analysis of the medium- and small-scale confinement. Three scales of confinement were present in the Pannonian Basin System. The basin-scale confinement of Lake Pannon developed due to pre- and synsedimentary deformation and resulted in frontally confined sandy depocentres at the end of basins. Confinement was significant near basin margins, while basin-floor areas could remain sufficiently unconfined for channel–lobe development. The basin-scale topography persisted until the slope progradation reached a given area, influencing its direction. Lateral basin margins coupled with the irregularity of the basin floor and frontal highs or sills promoted flow reflection, flow stripping and sand retention; representing the effects of medium-scale confinement. Medium-scale confinement also created topographically complex slopes, where deflected sandy channel fills and intraslope lobes were deposited in front of confining topography both related to a volcanic topography (Mezőcsokonya) and thrust-related high (Drava). This topography was healed before the arrival of the shelf-margin slope. The small-scale confinement includes the compensational stacking of lobes and channel-confinement.

Keywords: Pannonian Basin System, turbidite systems, confined turbidites, scales of topography

Introduction

Turbidite confinement has been studied in many basins around the world, as it can be a major control on sand distribution, and thus on hydrocarbon reservoir quality and architecture (Prather et al. 1998; Weimer et al. 2006). Effects of confinement can be captured on the turbidity current event scale, i.e. the bed scale, the architectural element, and the turbidite system scale. Scales are fundamental in geology, including sedimentology and structural geology. Structural geology can be fractal-like, similar patterns, geometries of deformation can be detected on different scales (Turcotte & Huang 1995). On the contrary, it has been proved that turbidite architecture is prone to be hierarchical rather than fractal-like (Straub & Pyles 2012; Cullis et al. 2018). Exploring the relationship between different basin geometries, sizes, and their effect on confinement could reveal crucial insights into sedimentary dynamics.

Turbidity currents, sediment gravity flows that are sustained by turbulence, are able to travel hundreds of kilometres on the basin plain. The basin floor topography can significantly alter the route of turbidity currents and thus modify the deposition of beds; this is termed as confinement (Lomas & Joseph 2004). The confinement of turbidity currents can be expressed in several ways on the event scale, e.g. ponding, reflection, deflection, deceleration, acceleration, flow decoupling, flow stripping, transformation into hybrid events (Kneller & McCaffrey 1999; Amy et al. 2004; Patacci et al. 2015, 2020). These processes may lead to thick mud caps, deflected routes and further sand deposition, sand dumping or erosion at the confining slope, separate sand and mud deposits, amalgamated sand beds, and muddy hybrid event bed (HEB) formation, respectively (Pickering & Hiscott 1985; Felletti 2002; Amy et al. 2004; Patacci et al. 2014; Dorrell et al. 2018). Confinement of successive turbidity currents can create high net-to-gross or upwards coarsening successions in the depocentres, sand bodies in peculiar positions, high lateral continuity of bedsets, multiple channel-levee transition zones (CLTZs) and tortuous corridors and channel fills (Sinclair & Tomasso 2002; Smith 2004; Sylvester et al. 2015; Brooks et al. 2018).

The Neogene Pannonian Basin System in Central Europe (Fig. 1) provides an excellent ground to study turbidite confinement and the processes controlling turbidite deposition (Juhász 1992; Sztanó et al. 2013b, 2016, 2026; Nyíri et al.

✉ corresponding author: Lilla Tőkés
lilla.tokes@ttk.elte.hu

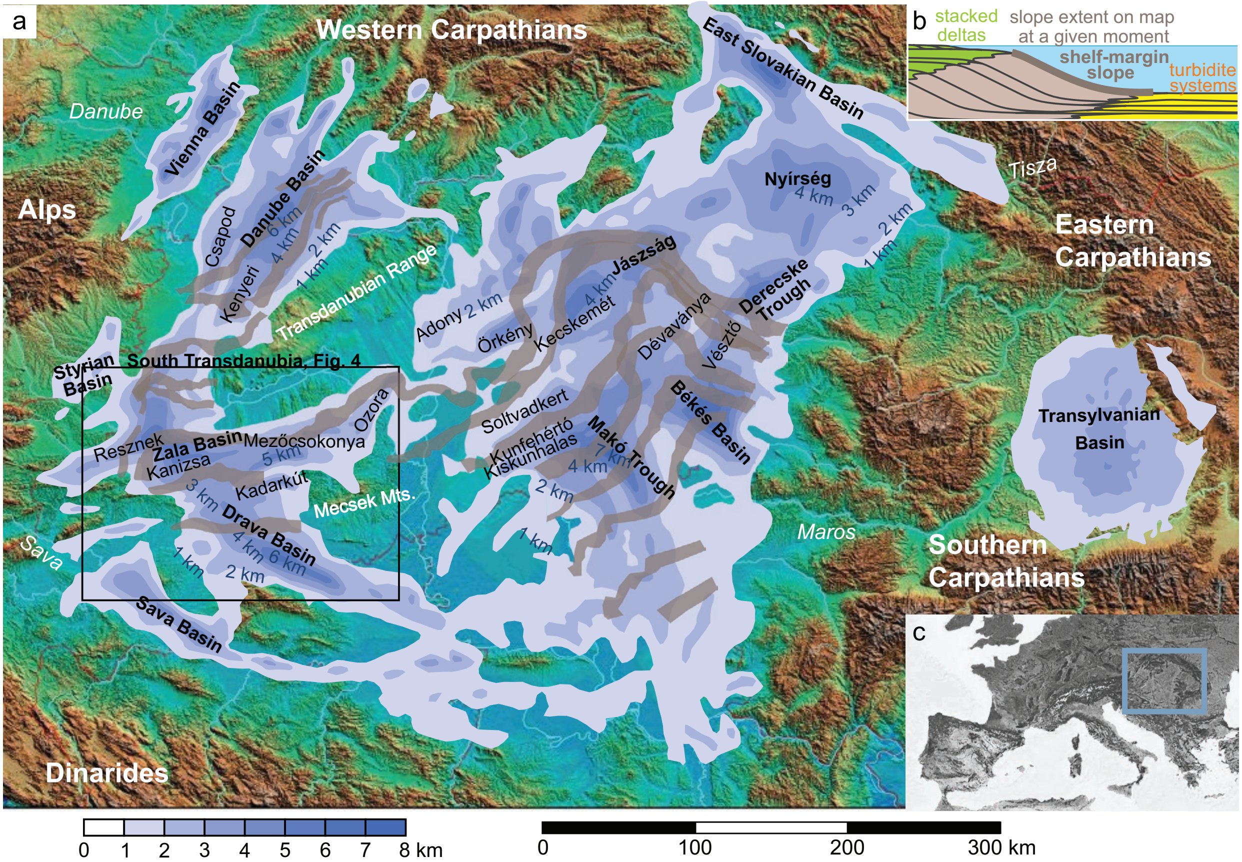

Fig. 1. (a) Basins of the Pannonian Basin System: Neogene thickness map and the position of the prograding shelf-edge slope, shown as grey bands (after Magyar et al. 2013). Note the irregularity and variety of basin shapes. Even though differential thermal subsidence, pre-, syn- and postsedimentary deformation altered the basement morphology, the overall geometry resembles the Lake Pannon basin floor at the time of turbidite deposition. The slope progradation direction and the axis of the subbasins is an important metric of the possible turbidite confinement. The main study area is the SW part of the Pannonian Basin System, South Transdanubia (Fig. 4); **(b)** Shelf-edge slopes are depicted on map as bands, showing their extent from the shelf-margin to the toe-of-slope at a given moment. Deltas develop on the shelf, turbidites are deposited at the toe-of-slope and further basinward. **(c)** Pannonian Basin System location in Europe.

2021). The back-arc basin system had an irregular topography, with up to 1000 m deep basins, submerged and emerged plateaus between them (Horváth et al. 2006; Törő et al. 2012; Sztanó et al. 2013b; Balázs et al. 2017) Advancing shelf-margin slopes provided a fairway for turbidity currents (Berczi & Phillips 1985; Juhász et al. 1994; Magyar et al. 2013; Sztanó et al. 2013b, 2026; Árgyelán et al. 2026).

The Pannonian Basin is also a well-known, prolific hydrocarbon province with several hydrocarbon systems (Horváth et al. 2015; Tari et al. 2023; Árgyelán et al. 2026). There are major reservoirs hosted in the Lake Pannon turbidite systems. Local factors played a role in hydrocarbon accumulation, such as inherited structures, syn- and postsedimentary deformation, sediment source, maturity, and confinement. Stratigraphic traps: onlaps, pinch-outs, facies change and structural traps: drape, compaction anticlines, high side fault with conformable upper seal have been identified, among others.

The sand distribution within the Pannonian turbidite succession is not only fundamental in hydrocarbon prospecting, but it is also of interest regarding groundwater flow patterns, geothermal resources, or CO_2 sequestration, H_2 storage (Falus et al. 2026; Gelencsér et al. 2026).

The aims of this paper are the following:

- Evaluation of basins of the Pannonian Basin System, especially in the SW Transdanubia, as confined turbidite basins;
- Investigation of the effects of topography on sand fairways and depocentres in the Southern Transdanubians;
- Differentiation of mechanisms of confinement and investigate their scale-dependency;
- Giving detailed examples of turbidite confinement, including the analysis of channel routes, lobe extension, paleotopography, tectonic control and the evolution of some confined basins.

Geological setting

Turbidites of the Late Miocene Lake Pannon were deposited in the Pannonian Basin, a large extensional basin system, surrounded by the Alpine, Carpathian, Dinaridic orogens

(Horváth et al. 2006). The extension started in the Early Miocene, characterized by large-scale detachments, smaller low-angle and high angle normal faults and transfer strike-slip activity (Fodor et al. 2017; Csontos et al. 2026). The extension was localised and dynamically migrated, leading to the successive opening of basins (Balázs et al. 2017), the youngest ones, like the Makó Trough, only started to open 11.6–9 Ma in Lake Pannon (Balázs et al. 2016).

A majority of the basins is approximately SW–NE oriented; however, there are a number of them quasi-perpendicular to these directions. The WSW–ENE trend in the central part is related to the strike of the Mid Hungarian Shear Zone; while basins with Early to Middle Miocene extension on the Tisza–Dacia unit showed NW–SE strike before Middle Miocene clockwise rotation (Balázs et al. 2017). The SSW–NNE trend in the NE part is due to the strike of detachment surfaces creating the basins (Tari et al. 1999). WSW–ENE Drava and Sava Basins are controlled by the strike of the Dinarides and the Sava suture zone (Ustaszewski et al. 2010). The NW–SE striking Makó and Szeged basins were the last to open, therefore reflect the last extensional directions (Balázs et al. 2017). The brackish water Lake Pannon is a successor to the marine Paratethys and formed when the uplift of the Carpathian orogenic belt separated its westernmost portion (Magyar et al. 1999). The Pannonian Basin System was fed by two large river systems from the Alps and Carpathians, the Paleo-Danube from the NW and the Paleo-Tisza from the NE. Fluvial, deltaic, shelf-edge clinoform (Algyő Fm), turbiditic (Szolnok Fm) and hemipelagic (Endrőd Fm) environments developed in the subsiding lacustrine basin system (Juhász 1992; Sztanó et al. 2013a, b). The prograding paleoslope gradually filled Lake Pannon (Magyar et al. 2013; Balázs et al. 2018; Magyar 2021). The inherited topography influenced the direction of slope progradation and the shape of the several hundred metre-high clinothems (Uhrin et al. 2009; Törő et al. 2012).

Aggradation and progradation of the shelf-edge alternated, due to climatic variations. During humid periods, the base level rise and high sediment supply meant that the clinothems aggraded and efficient turbidity currents deposited in detached lobes. During base level stagnation, shelf-edge progradation took place and the sandy, low volume turbidity currents deposited attached toe-of-slope lobes (Sztanó et al. 2013b).

Three turbidite systems existed in Lake Pannon: (1) unconfined toe-of-slope turbidite system fed by inefficient sandy turbidity currents (Mutti 1999); (2) unconfined slope-related turbidite system with channel-levee systems, lobes and tortuous corridors; and (3) confined deep basin centres fed by efficient muddy turbidity currents (Sztanó et al. 2026). In the latter, thick, tabular lobes, onlaps, backstepping lobes, deviated channels, filled mini basins have been found. Tabularity on the lobe-scale has been presented in the Makó Trough: individual lobes within 50–150 m thick lobe complexes can be correlated for up 10–30 km (Sztanó et al. 2013b; Tőkés & Patacci 2018). The high net-to-gross and larger thickness of lobes and lobe complexes compared to other basins suggests confinement, and reflection of flows, at least at the far end of the basin (Sztanó et al. 2013b).

Methods

Seismic geomorphology and subsurface sedimentology

The potential confined basins of the Pannonian Basin System, and well-known analogues are compared based on their geometrical relations, including their size and direction. Sand distribution is studied on maps from the literature, the sand percentage of the Szolnok Fm was based on semi-quantitative sand-mud interpretation of spontaneous potential and resistivity well-logs (Fodor et al. 2013). This gives an average net-to-gross of the whole turbiditic interval, excluding the shelf-margin slope, that shows us the areas of preferential sand accumulation.

Published 2D seismics offer overview on the rarely studied turbidites and allow quantitative comparison of basins and scales of topography. Reflection thickness is used as a proxy for the thickness of the sediment package on the upstream and downstream sides of high; measured in milliseconds, as local time-depth data were not available. The height of confining margins was estimated based on regional time-depth data, without decompaction. This gives a large margin of error, that is why only three groups were created in Fig. 2.

3D seismic cubes were analysed to reconstruct the paleotopography and geomorphology of the region; the channel routes; the location, downlap or onlap relations, the stacking of lobes, the evolution of the system, the effects of confinement, the sand-mud distribution, and the spatial distribution of reservoir characteristics. Flattening of seismic sections onto a paleohorizontal surface, represented by a delta plain horizon was used to remove post-rift differential thermal subsidence and neotectonic deformation to understand the paleotopography of the area (Sztanó et al. 2007). This method does not account for compaction or deformation between the deposition of the first turbidites and the delta plain horizon. Seismic reflection facies, reflection terminations, lateral amplitude variations and amplitude maps of horizons allow geomorphological interpretation. Spectral decomposition with Fast Fourier Transform was done, frequency ranges for RGB blending were selected based on the notches on the frequency histogram and based on clearest channel morphologies. The vertical resolution is approximately 25 m at the depth of 2–3 km. Well-logs were tied to seismic sections using standard VSPs and check-shots. Spontaneous potential, gamma ray and resistivity logs were correlated. A single well core was studied by facies analysis.

The sinuosity of deepwater channels tells us about the slope profile vs the equilibrium profile of the flows (Pirmez et al. 2000; Kneller 2003). The equilibrium profile that the channels tend toward, is determined by flow parameters: density, thickness, grain size distribution. Above grade channels are erosional and straight, at grade channels are highly sinuous and migrate laterally, whereas below grade channels are sinuous but aggrade and build levees. When flows become more efficient, i.e. muddy, high volume and/or high density, their equilibrium profile shifts, the gradient is reduced, and erosion is prevalent (Kneller 2003). When the erosional base of flows shifts to a downstream basin, the currents become above grade at the barrier and incise into it (Sinclair & Tomasso 2002).

3D seismic and well data were provided by HHE North Ltd. and Magyar Horizont Energia Ltd. The interpretation of horizons, and flattening was carried out in S&P Global (IHS) Kingdom software. Spectral decomposition was achieved in dGB Earth Sciences OpendTect software.

Basin sizes of the Pannonian Basin System

There are 12 major basins and plenty of minor basins in the Pannonian Basin System (Fig. 1). Some of them are subbasins of major basins or are discrete smaller basins. The present-day depth map of the Neogene basement (Fig. 1) resembles the topography that the turbidity currents encountered and was used as approximation for the geometry of the basins. In order to shed light on the variety of basin morphologies and sizes, basic basin characteristics will be discussed. The size of the basins (Fig. 2) controls the degree of confinement; it determines whether the turbidity currents can spread across the basin floor or they are confined by the basin margins (Southern et al. 2015). Since the dominant turbidite sand sizes are very fine, fine grained all across the basin system, and the log patterns are similar as well (Juhász 1992; Uhrin & Sztanó 2012; Sztanó et al. 2013b, 2016), it is postulated that there was not significant spatial variation in the average size of turbidity currents. This means that they behaved similarly when encountering similar basin shapes and sizes regardless of time and space. An exception could be the Transylvanian Basin where medium- to coarse-grained turbidites are common, as well as gravelly turbidites; however, their sources were much closer than in the rest of the basin system.

The 12 major basins and 18 selected minor basins were measured on the base map, based on their significance in the turbiditic fill and roughly definable margins (Fig 2a). Basins from the detailed 3D seismic studies (Mezőcsokonya and Drava) were also added. The dip length of basins refers to the axis of the basin that is closer to the direction of incoming turbidity current, the strike length is the perpendicular axis.

Fig. 2. (a) Aspect ratio (dip:strike length) and area of selected basins of the Pannonian Basin System. The dip length represents the axis of the basin closer to the direction of incoming turbidity currents (based on slope progradation direction); the strike length is the perpendicular axis. Depth of basins (shallow, deep, very deep) describes the approximate, compacted height of the frontal basin margin that was opposite to the incoming flow. Backstripped, decompacted heights would be needed for a more accurate analysis. Note the logarithmic scale on both axes. GBH N, S: basins on Drava 3D (Fig. 4 – B) north and south of Görgeteg–Babócsa High. **(b)** The aspect ratio (dip:strike length) and area of famous confined basins compared to Pannonian basins. Note the logarithmic scale on both axes.

Paleoflow was assessed from the prograpdation direction of shelf-margin slopes 20–30 km away from the basin, since the Szolnok Fm turbidites were detached from the toe-of-slope (Sztanó et al. 2013b).

There are larger than 80×80 km (~5000 km^2), and smaller than 5×10 km (~40 km^2) basins. Isometric basins (e.g. the Resznek, Békés, and Adony Basins) have an aspect ratio around 1; elongated basins are closer to 0.1 if they are frontally confined, or 10 if they are laterally confined. The incidence angle of paleoflow can be around 45° with respect to the longer axis; in theses cases, the data points can be on either side of 1 on the y axis of the diagram. E.g. Csapod and Kenyeri Troughs are quasi-parallel neighbouring basins, and received paleoflow from similar direction, but a 10° difference in incidence angle means they are shown as laterally and frontally confined, respectively.

Kecskemét and Mezőcsokonya Basins are good examples of troughs with high incidence angles where turbidity currents were most probably frontally confined, reflected and/or deflected. Dévaványa and Makó Basin are similar shaped troughs; however, turbidity currents could run across the basin axis and only encountered lateral confinement until the flows reached the frontal end of the basin. This is greatly exemplified by the Makó Trough asymmetric channel that had more developed, long wavelength curves on the dip side, while sharp, short curves on the upper side of the lateral slope (Sztanó et al. 2013b). The currents decelerated, deflected on the lateral slope, creating the sharp turns, while their downslope acceleration created the wider curves (Sztanó et al. 2013b).

The roughly estimated depth of basins on the frontal margin, or the height of the sill acting as frontal confinement, based on published 2D seismics, (Fig. 2a) suggests how confining the basin was for flows that reached the margin: the lower than 200 m margins are usually smaller than the stratigraphic thickness of turbidites: they probably influenced deposition, but not throughout the turbidite succession. The 200–500 m high margins are on the scale of the stratigraphic thickness of turbidites in many basins; while the deeper basins must have contained all turbidity currents and probably influenced slope deposition. Basins with small areas (eastern, western, GBH S and N) can be relatively deep (200–500 m) as well.

To find analogues around the world, 45 basins from 14 famous confined turbidite locations were compared with the Pannonian ones (Fig. 2b). Not only separate basins, but also temporal shifts in basin size were included. The Gulf of Mexico salt-withdrawal minibasins (Prather et al. 1998) and the basins of the Annot Sandstones (Smith & Joseph 2004) are smaller than the major basins of the Pannonian Basin System. The minor basins are in the range of the common confined basins, and the largest major basins have only a few counterparts. The 5000 km^2 Austrian Molasse is an axially confined conduit where lateral seismic onlap and low sinuosity and slow lateral migration of channels records confinement (Covault et al. 2009). The 4500 km^2 Marnoso Arenacea Foredeep depicts ponding of high volume highly efficient flows (Amy & Talling 2006).

Sandy depocentres in the Zala Basin and adjacent areas: basin- and medium-scale confinement

Net-to-gross, thickness and onlap relationships

The average net-to-gross data and the thickness of the turbidites is a good measure of the type and degree of confinement. For this analysis, the grid data of Fodor et al. (2013), covering the Zala Basin, provide a perfect opportunity. The Zala Basin is in the vicinity of the detailed study areas of confinement of this paper, a variety of structures and basin shapes are present, and the shelf-edge slope progradation is well constrained in the greater area (Uhrin et al. 2009; Törő et al. 2012). The term Zala Basin generally includes the Resznek Basin N of the Budafa–Lovászi Anticlines, and the Kanizsa Basin S of them.

The average net-to-gross of turbidites, based on well logs (Fodor et al. 2013), was overlain on the base turbidite depth map in greyscale (Fig. 3a). The sand net-to-gross ratio is depicted by yellow colours, less than 50 % sand has 50 % transparency, and less than 30 % sand is fully transparent to show the topography. The progradation of the shelf-edge slope was documented by Magyar et al. (2013; polygons) and by Uhrin et al. (2009; arrows). The location of oil and gas fields in the Szolnok Sandstone (Selmeczi 2018) is also indicated on the turbiditic Szolnok Formation thickness maps (Fig. 3b).

The highs and lows of the paleotopography were similar to the present-day depth map (Fig. 4); however, their degree of elevation difference was much smaller. The Transdanubian Range has uplifted 600–700 m since the Late Miocene (Ruszkiczay-Rüdiger et al. 2020). The anticlines of the Zala area – Budafa, Lovászi, Kilimán (Ortaháza), Belezna (Inke) were active in the early Pannonian, indicated by onlaps, thinning and fining of the turbiditic interval towards the highs (Fodor et al. 2013). Árgyelán et al. (2026) suggest a quiescent phase during turbidite deposition. This means that the antiform topography was present, albeit only on the scale of 50–200 m.

The Budafa–Lovászi Anticlines did not influence the thickness or the overall progradation direction of shelf-edge clinothems (Uhrin et al. 2009; Table 1). In contrast, a slope did not develop above the axis of the Belezna Anticline, indicating that the uplift was ongoing (Uhrin et al. 2009). Direction of progradation of the slope was also influenced by Kilimán Anticline (Majercsik 2009; Skorday 2010). The deformation of the anticlines was the most active after the shelf-edge progradation and continued until the Quaternary (Uhrin et al. 2009). Inversion was outpaced by thermal subsidence, but altered the basin floor topography (Oravecz et al. 2024; Balázs et al. 2026).

The Kilimán, the Budafa and the Belezna Anticlines contain well studied, prolific hydrocarbon fields. The Kilimán Anticline is a compaction anticline, but depositional facies change also plays a role in some of the fields (Árgyelán et al. 2026). Budafa is regarded as a drape anticline. Most of the hydrocarbon fields, as expected, are on structural highs due to migration and structural trapping. However, the question arises whether the structural predetermination of sedimentary processes played a role in reservoir characteristics and the stratigraphic pinchouts.

Six depocentres have been identified where the basin-floor turbidites have increased net-to-gross relative to the surrounding areas (45–80 % maxima, Fig. 4, Table 1). Their characteristics will be discussed from the aspect of potential confinement. The slope progradation is predominantly N-to-S, suggesting a northerly source for the turbidity currents. Four sandy depocentres (1, 2, 3, 4 on Fig. 3a, Table 1) are close to the N–S trending margin of the Transdanubian Range. The extent of the depocentres is 5–10 km, they do not correspond to individual basins or subbasins identifiable on the scale of the depth map. Depocentres 1 and 3 are in recesses of the basin margin (Fig. 3b). Depocentre 2 is on a topographic nose and continues towards the south where another recess is present. This depocentre is the place where the confluence of two shelf-edge slope lobes occurred, coming from the Csapod and Kenyeri Troughs, going around the Mihályi High from its two sides (Uhrin 2011). The stratigraphic thickness of the basin-floor turbidites is not higher in the discussed depocentres (1, 2, 3, 4) than at the surrounding areas (Fig. 3b). Depocentre (4) is upstream, N of the axis zone of the Kilimán High. The part of the Kanizsa Basin that is S of the Kilimán High is significantly muddier than the rest of the Zala area (<40 % sand).

The Resznek and Kanizsa Basins are the deepest basins in the area, which is reflected by the thickness of the turbidites. In the Resznek Basin, the highest net-to-gross (55 %; depocentre 5) is not in the deepest part, but on a small plateau on the upstream, northern flank of the Lovászi Anticline. There is a decrease in net-to-gross towards the axis of the anticlines. In the Kanizsa Basin, the deepest depocentre corresponds to the highest sand ratio. At the northern flank of the Belezna Anticline (6), there is a slight increase in net-to-gross before a steady decrease, paired with a thinning to less than 200 m. Depocentre 6 (Fig. 3b) is near the gas fields, but does not correspond to them. The known fields on the anticline are in relatively muddy turbidite units (25–45 % net-to-gross).

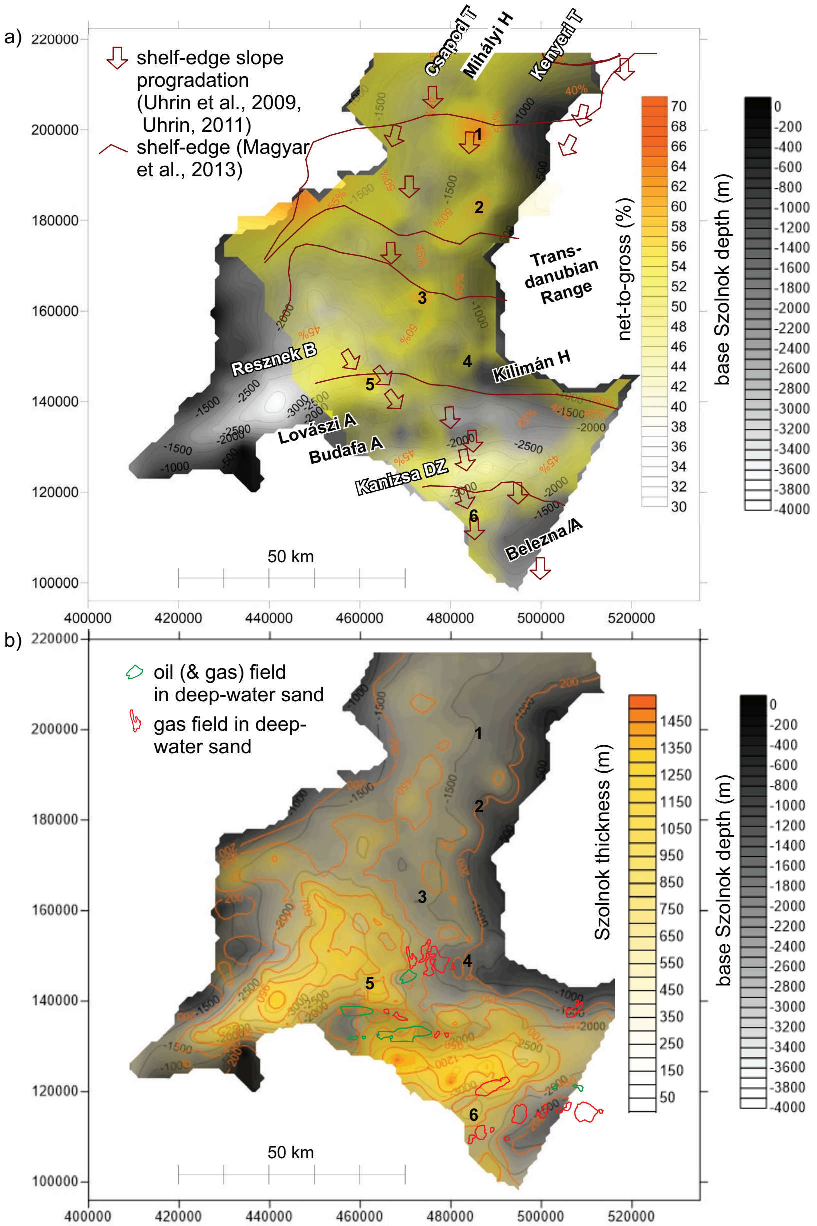

Fig. 3. Turbidite distribution in the Zala Basin. **(a)** Turbidite base depth and average turbidite net-to-gross (Fodor et al. 2013), coupled with slope progradation direction and clinoform planform shape (based on Uhrin et al. 2009 and Magyar et al. 2013). Main anticline names are depicted with black, and basins with white. Numbers depict depocentres discussed in the text, depocentres 1–5 have >55 % sand. **(b)** Turbidite thickness in the Zala Basin. Turbidite base depth, turbidite thickness (Fodor et al. 2013), and oil and gas fields in the Szolnok and Algyő Formations (Selmeczi 2018).

Onlaps have been found to be the only common evidence that is present in all confined basins globally, regardless of size and mechanism of confinement (Prather et al. 1998; Kneller & McCaffrey 1999; Haughton 2001; Smith & Joseph 2004; Covault et al. 2009; Etienne et al. 2012; Tinterri & Tagliaferri 2015; Marini et al. 2016; Liu et al. 2018; Tőkés & Patacci 2018). 2D sections show that there is significant onlap of turbidites from the direction of slope progradation, pinching out towards the south, on the Kilimán and Belezna Highs (Fig. 5a, c). In both cases, the thickness of the turbidites decreases significantly, to less than 200 m based on the thickness map (Fig. 3b), or to less than around 50 m based on the seismic sections (Fig. 5a, c). There are onlaps on the steep southern side of the Kilimán High as well, but the seismic reflections are thinner on the southern side (20 vs 30 ms, 50 m from onlap), while the turbiditic packages are similar in thickness on the two sides. The turbidites above the Budafa Anticline are significantly thinner than next to it. Only a few onlaps can be detected on these seismic sections (Fig. 5a, b). The turbidite reflection package that continues above the anticline thins significantly, by ~80 ms, above the anticline. Onlaps on the southern side continue in thinner reflections (25 ms) than reflections on the northern side (38 ms).

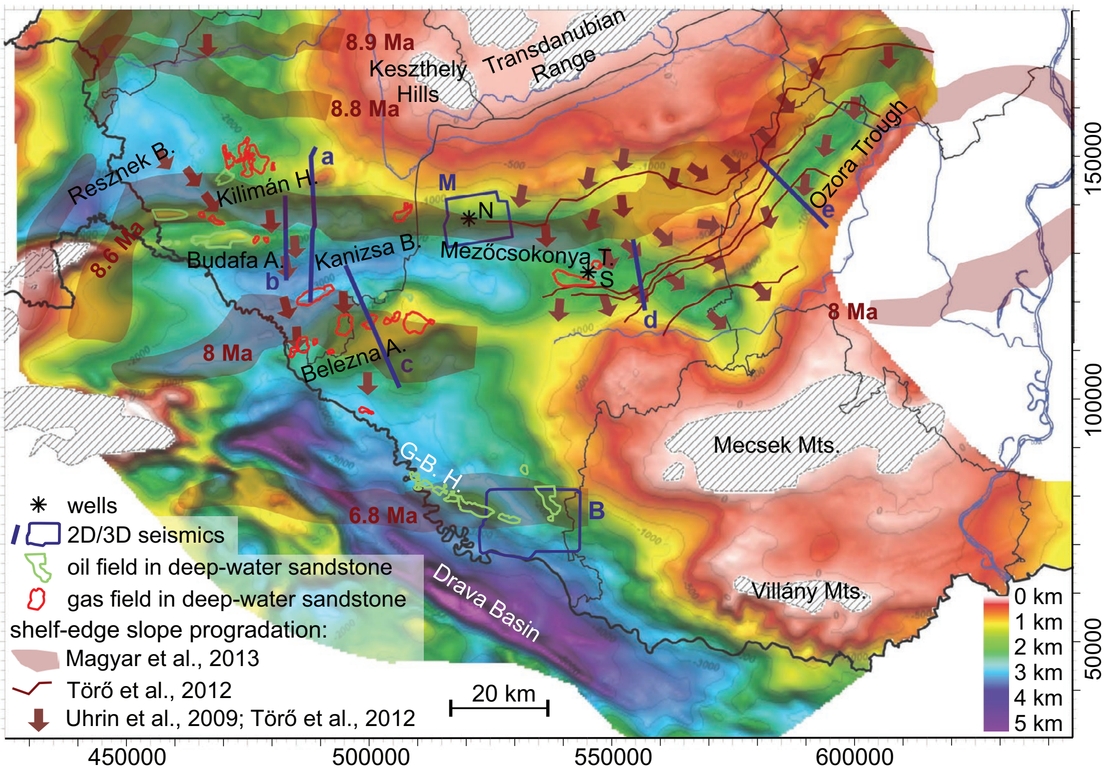

Fig. 4. Pannonian base map of SW Transdanubia (Horváth et al. 2015), showing the progradation of the shelf-edge slope (Uhrin et al. 2009; Törő et al. 2012; Magyar et al. 2013), the location of hydrocarbon fields in the deep-water sandstone, the location of the 2D seismic sections (Fig. 5a, b, c, d, e) the location of the 3D seismics (M: Fig. 7b, B: Fig. 10a) and the location of N (Northern) wells, and S (Southern) wells (Fig. 6; Gyetvai 1999). G-B. H.: Görgeteg–Babócsa High.

Table 1: Sand depocentres in the Zala area and characteristics suggesting acts of confinement, such as pinch-out against a confining high, sand retention via flow stripping. The distance of the centre of the sand depocentre to the axis of the ridge and to the related hydrocarbon field shows that the depocentres are usually upstream of the ridge and the hydrocarbon fields are located in between the centre of the depocentre and the axis of the ridge. This is probably due to the pinch-out geometry and thinning of beds towards the ridge.

	Location	Slope progradation affected	Number of onlaps up-stream of high	Net-to-gross			Thickness of turbidites			Thickness of individual reflections		Distance to ridge axis/ *HC field*
				Upstream of high; max	On high; max	Downstream of high	Upstream of high	On high	Downstream of high	Upstream of high	Downstream of high	
1				65 %		45 %	250		300			0 km/n.a.
2				60 %		45 %	300		400			8 km/n.a.
3				58 %		45–55 %	350		450			2 km/n.a.
4	Kilimán	direction	4	50 %	50 %	28–40 %	400 m	50–250 m	700 m	20 ms	30 ms	4 km/*2 km*
5	Lovászi-Budafa	no	2	58 %	45 %	40–50 %	1000 m	650 m	1300 m	38 ms	25 ms	7 km/*7 km*
6	Belezna	thickness	4	52 %	45 %	20–40 %	700 m	50/300 m	150 m			6 km/*3 km*
	Mező-csokonya	thickness, direction	4	80 %			400 m	0 m				10 km/*2 km*

The Mezőcsokonya Trough also shows onlapping relationships on its southern side, where even prograding shelf-edge slopes were deflected in response to the topographic barrier (Fig. 5d; Törő et al. 2012). The continuous reflections become more disordered approaching the downstream high. Most onlaps are on the high, but a few onlaps are 100–200 m away from the slope. The Ozora Trough onlaps show even more scattered onlaps, only about half of the reflections are close to the downstream high, the others pinch out 2–3 km basinward from the margin (Fig. 5e).

Two suites of well log data were taken from the upstream and downstream ends of the Mezőcsokonya Trough (Figs. 4, 6). The upstream wells are on the Mezőcsokonya 3D seismic block, the downstream wells are located in the SE end of the Mezőcsokonya Trough, close to some gas fields (Fig. 4; Selmeczi 2018). One of the latter (Mezőcsokonya Field) is on a 3-way-closed antiform, the fourth side is closed by a high-side fault (Árgyelán et al. 2026). The two suites of wells are 30 km away and are probably hard to correlate. However, they show the common characteristics of turbidites on the upstream and the strongly confined downstream parts of the system.

The deep lacustrine marl (Endrőd Fm.) is only 10–20 m thick in the upstream wells, but 50–100 m thick in the downstream wells. 5–10 m thick sand units with serrated log pattern and up to 50 m thick blocky or upward coarsening then upward fining sand units are common in the upstream wells. Correlation of well logs was based on the 3D seismics which showed common channel-form bodies both in section and in map view. The sand bodies are not continuous, and even if they are, they change in character considerably, e.g. from upward coarsening to blocky serrated log pattern.

The downstream wells were correlated using only the well logs. 50–100 m thick sand bodies – separated by 10 m thick shales – look continuous over 1–2 km, their character and thickness changes slightly in adjacent wells. 5–10 m thick upward coarsening or fining units are often amalgamated; make up 20–40 m thick units separated by few m thick that-make up the 50–100 m thick sand bodies.

Interpretation

The net-to-gross distribution in the Zala Basin can be explained by topographical effects. On an even basin floor, the sandiest depocentres would show a well spread out, even thickness (Groenenberg et al. 2010; Terlaky et al. 2016). They could be attached to or detached from the toe-of-slope

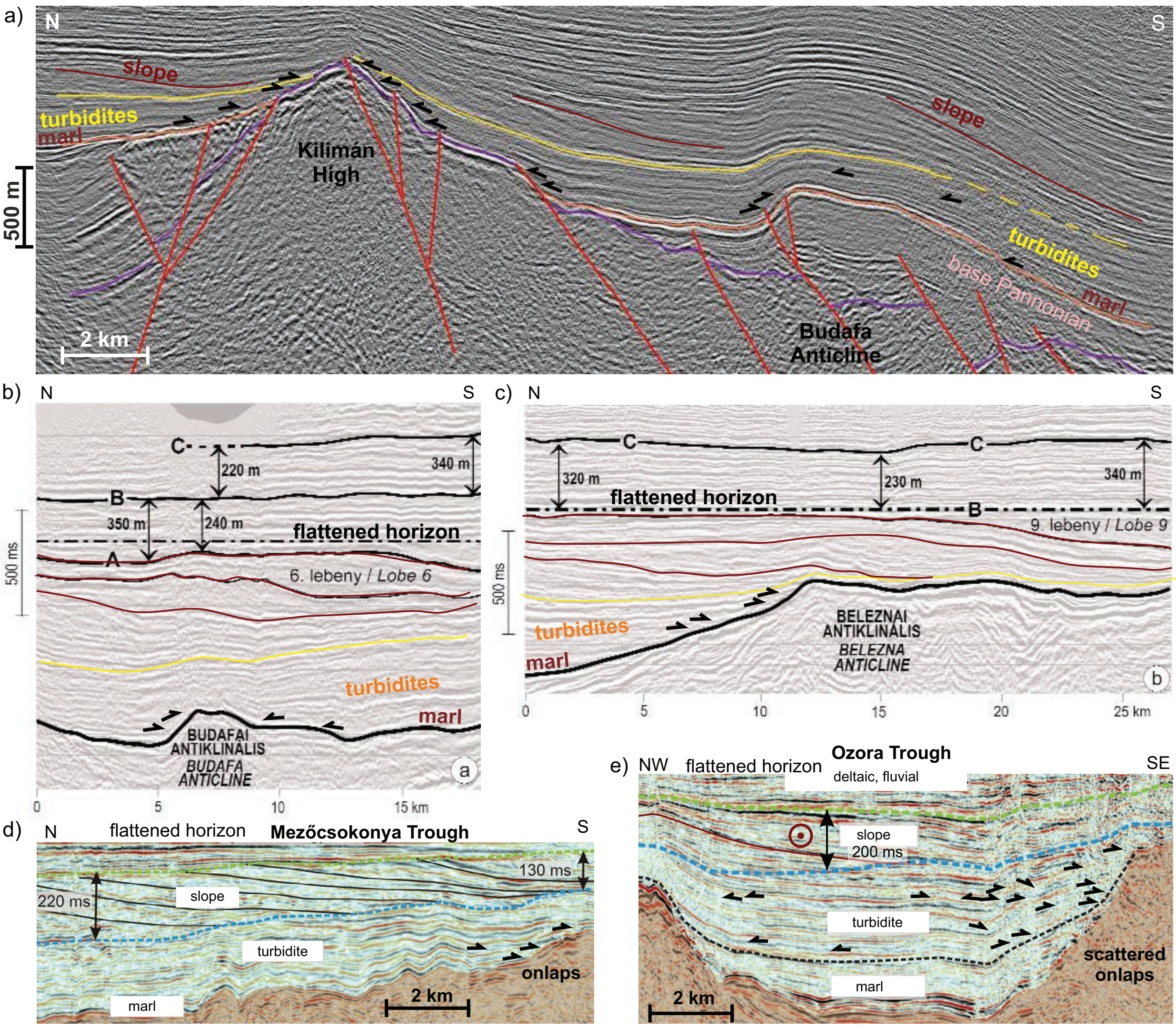

Fig. 5. Published 2D sections showing onlaps onto the basin highs, the most common evidence of confinement Location on Fig. 4. **(a)** Section across the Kilimán High and the eastern end of Budafa Anticline (Kovács & Gyuricza 2015). **(b)** Flattened section onto a paleohorizontal deltaic reflection, across Budafa Anticline (Uhrin et al. 2009). The turbidites are thinner above the anticline and there are a few onlaps in the lower reflections. **(c)** Flattened section onto a paleohorizontal deltaic reflection, across Belezna Anticline (Uhrin et al. 2009). Almost all turbidites onlap onto the anticline. **(d, e)** Onlapping relations on the downstream margins of elongated troughs.

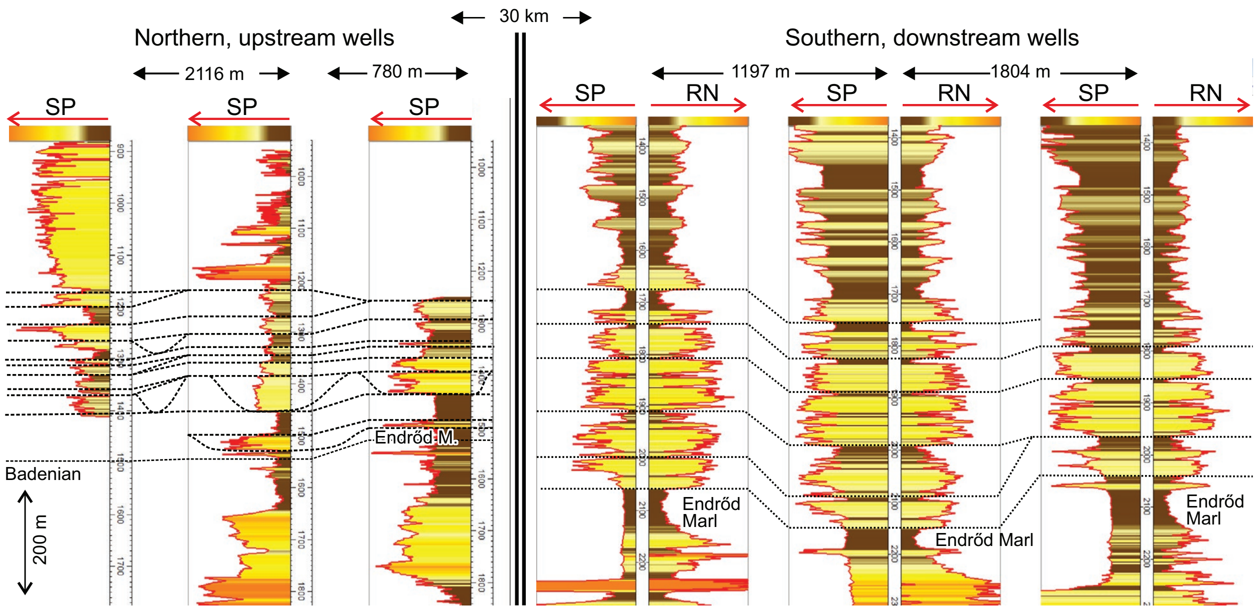

Fig. 6. Well log correlation (SP – spontaneous potential, RN – resistivity) at the upstream northern margin and the southern confining margin of the Mezőcsokonya Trough (Fig. 4: N and S). Correlation of the upstream wells was based on seismic reflections. Note the channel-form bodies and pinch-outs. Downstream well data were taken from Gyetvai (1999). The turbidite bodies can be easily correlated between sections 1–2 km away.

depending on their efficiency (Mutti 1999; Van der Merwe et al. 2014), and their lateral extent would depend on the number of feeder channels . This is not the case of the Zala Basin, with unique sandy depocentres strongly connected to changes in topography.

The sandy depocentres 1, 2 and 3 were confined laterally by the eastern basin margin and frontally by the noses in the margin to the S of them. The spreading of the turbidite lobes was stopped by the lateral margin, which happened all along the margin, but the additional frontal barrier or sill caused deceleration of the turbidity currents and dumping of the sand in the depocentres. Depocentre 2 sits on a nose, its interpretation needs a more thorough study. The confluence of two lobes coming from the Csapod and Kenyeri Troughs could explain its location (cf. Uhrin 2011) or backstripping of the postdepositional deformation could clarify its origin.

The onlaps of the sandy depocentre in front of the Kilimán High (4) show that flows were reflected/deflected and did not surmount the high. Since the Kilimán High does not reach far into the basin centre, and the sandy depocentre extends towards its W, it is possible that some flows went around it. The thinner reflections on the downstream side and the low sand content in the downstream basin (Kanizsa) suggest strong flow stripping and prolonged bypass. The steep southern gradient could accelerate the flows to such a degree that the sandy flows ran across the basin and only the muddier tail deposited in their wake (Prather et al. 1998; Stevenson et al. 2014; Soutter et al. 2021).

Depocentre 5 in front of the Lovászi Anticline, away from the basin centre, developed due to the frontal confinement of the anticline. The turbidity currents could spread across the Resznek basin floor, and surmount a slight topography, but the anticline was high enough to cause decelerational dumping of sand. Even though the Lovászi and Budafa Anticlines have just started their activity and only presented a small height difference (Uhrin et al. 2009), they created a sandy depocentre upstream of them, and thinning, fining and a few pinchouts towards their axes. The reflections that are thick on the upstream and thin on the downstream side of Budafa Anticline indicate that the sandy units become thick and tabular approaching the high, a common occurrence in confined turbidites, resulting from flow reflection and/or flow stripping. The southern side acted as a downstream basin, where the thin beds could also be a result of flow stripping, whereby the sandy lower parts of flows were reflected in the upper basin and only the muddy upper parts reached the downstream basin (Sinclair & Tomasso 2002). Bypass with minor deposition is also common on the downstream slopes since the gradient of the slope leads to acceleration of turbidity currents. A local supply system reaching the basin from the W (Juhász et al. 1994; Fodor et al. 2013) could also contribute to the difference in turbidite character.

Depocentre 6, north of the Belezna Anticline, was also a result of frontal confinement. Based on onlaps, most turbidity currents could not surmount the slope due to the significant height of the barrier. The high was so shallow that the slope could not develop on top of it, only a gently inclined ramp prograded over it (Uhrin et al. 2009). A more significant sandy depocentre could be expected based on the height of the confining margin Without flow stripping, the sand and mud are both dumped, leading to a relatively low (25–45 %) net-to-gross. It is also possible that sandy depocentres only developed locally, in response to gradient changes, or the reservoir sandstones only developed in certain depths of the turbidites.

The aggradational onlaps of the Mezőcsokonya Trough are common on strongly confining, but low gradient slopes, where the flow deposits progressively heal the topography (Spychala et al. 2017b). In contrast, the steeper margin of the Ozora Trough created scattered onlaps. The slope prograded towards the SE before reaching the N–SW trending Ozora Trough which diverged the slope progradation towards the S (Törő et al. 2012). The earlier arriving basin-floor turbidity currents likely experienced the same fate; they were frontally confined and reflected or deflected by the SE margin. The scattered onlaps suggest that some suits of turbidity currents reached the margin and were reflected/deflected, but left a bulge of sediment at the toe of the margin due to rapid deceleration, leading to earlier deflection of successive flows (Soutter et al. 2021). Abrupt sediment fallout and bed thickening towards the laterally confining slope has been linked to slow, highly depositional flows (Amy et al. 2004). This can happen to the already diverted flows in the Ozora Trough.

The upstream, northern well logs of discontinuous channel fills are typical toe-of-slope turbidites, belonging to the Algyő Formation (Sztanó et al. 2013b). The thinner, non-channel like units that change facies or pinch-out between wells can be intraslope lobes or levees. The small topographical differences in the area will be discussed in the next section. The continuous thick sand bodies of the downstream well logs are typical basin-floor turbidites (Juhász 1992; Amy & Talling 2006; Sztanó et al. 2013b; Fonnesu et al. 2018). The 5–10 m thick sand units can be lobe elements, the 20–40 m thick units lobe complexes, and the 100 m thick ones lobe complex sets or systems (Sprague et al. 2005). Their tabularity and a few pinch outs can be attributed to confinement, their sandy nature might imply flow decoupling and sand dumping (Kneller & McCaffrey 1999; Felletti 2002), but a more thorough comparison with basin floor lobes on the unconfined part of basin is needed for certainty.

The characteristics of confinement – sandy depocentres, pinch-outs, flow stripping, effect on slope progradation – are similar in the studied cases, but their degree has variations across confining highs. It is a question whether we consider the Zala Basin as one basin with smaller sills, highs, or we consider the Resznek, Kanizsa Basin and the basin north of Kilimán High as separate basins. We argue that even though the Kilimán High altered slope progradation and the turbidites pinch-out completely on the eastern part of the ridge, turbidity currents could surmount most of it or flow around the ridge, it did not seal off the basin completely. The topography of the Budafa–Lovászi Anticlines was healed relatively easily. The Belezna Anticline, on the other hand, could be regarded as a strong frontal margin, that even confined the slope from developing to its potential height. In this sense, Zala Basin, Mezőcsokonya Trough and Ozora Trough represent basin-scale confinement, while the rugosity of the basin floor is on the medium-scale.

Evolution around a volcanic high, Mezőcsokonya: medium- and small-scale confinement

The basin-scale confinement exemplified by the Zala Basin and adjacent areas were studied based on regional maps and 2D sections. Its effect could also be studied on 3D seismics, but the location is crucial: the blocks need to be along the confining margin, preferably at sandy depocentres identified on the net-to-gross map (Fig. 3), and possibly covering part of the downstream basin as well.

Other 3D seismics, especially ones with a rugged basin floor, are perfect for studying the possible effects of smaller scale topography. Two 3D seismic datasets will be discussed, both on the upstream ends of large basins: one on the northern side of the Mezőcsokonya Trough, and one on the northeastern side of the Drava Basin (Fig. 4).

Paleotopography and structural control

The Mezőcsokonya Trough is a major (30×70 km) NW–SE trending basin (Fig. 7a). The current Base Pannonian topography shows that the Mezőcsokonya Trough is 1.5–2 km deeper than its neighbourhood (Fig. 7a), while the flattened paleotopography shows around 800 m difference in depth between the trough and the surrounding highs, without decompaction (Fig. 7b, Törő et al. 2012).

The paleoslopes reached the area from the NNW, prograding southwards (Fig. 4; Törő et al. 2012). There are no seismic-scale shelf-margin paleoslopes N of the Mezőcsokonya Trough, which could have been contemporaneous with the turbidites, but deltas prograded over the Balaton Area (Sztanó et al. 2013a). Paleoslopes only developed in the North Zala area. The easternmost slopes were dipping S, towards the troughs, away from the Bakony–Balaton Highlands which were first exposed as a high and later flooded during the early Late Miocene (Csillag et al. 2010; Sztanó et al. 2013a, 2020, 2026; Fodor et al. 2021). The shallow parts of the lake in the area of the Bakony–Balaton Highlands were rapidly filled, then deltas (10–50 m thick) could supply sediment towards the Mezőcsokonya Trough. The turbidites were most likely deposited between 9–8.6 Ma, when the slope was sufficiently close, less than 60 km away, but the slope has not yet advanced over the area.

The studied 3D cube (Fig. 4 – M) is on the upstream side of the Mezőcsokonya Trough (Fig. 7a). The paleotopography of the trough was irregular, with ridges 0.5–2 km apart (Fig. 7b, d). The basin floor shows a topographic high in the middle of the cube (north of the Mezőcsokonya High), separating a small northern subbasin, a small western subbasin and an eastern one that probably continues towards the Mezőcsokonya Trough. The extent of this topographic high is 7 km in an E–W and 4 km in a N–S direction. The lows are in the range of 3–5 km across, their continuation towards the W (Kanizsa Basin) or E (Mezőcsokonya Basin) is uncertain.

The topographic highs in the middle of the 3D volume correspond to a Lower–Middle Miocene volcanic structure

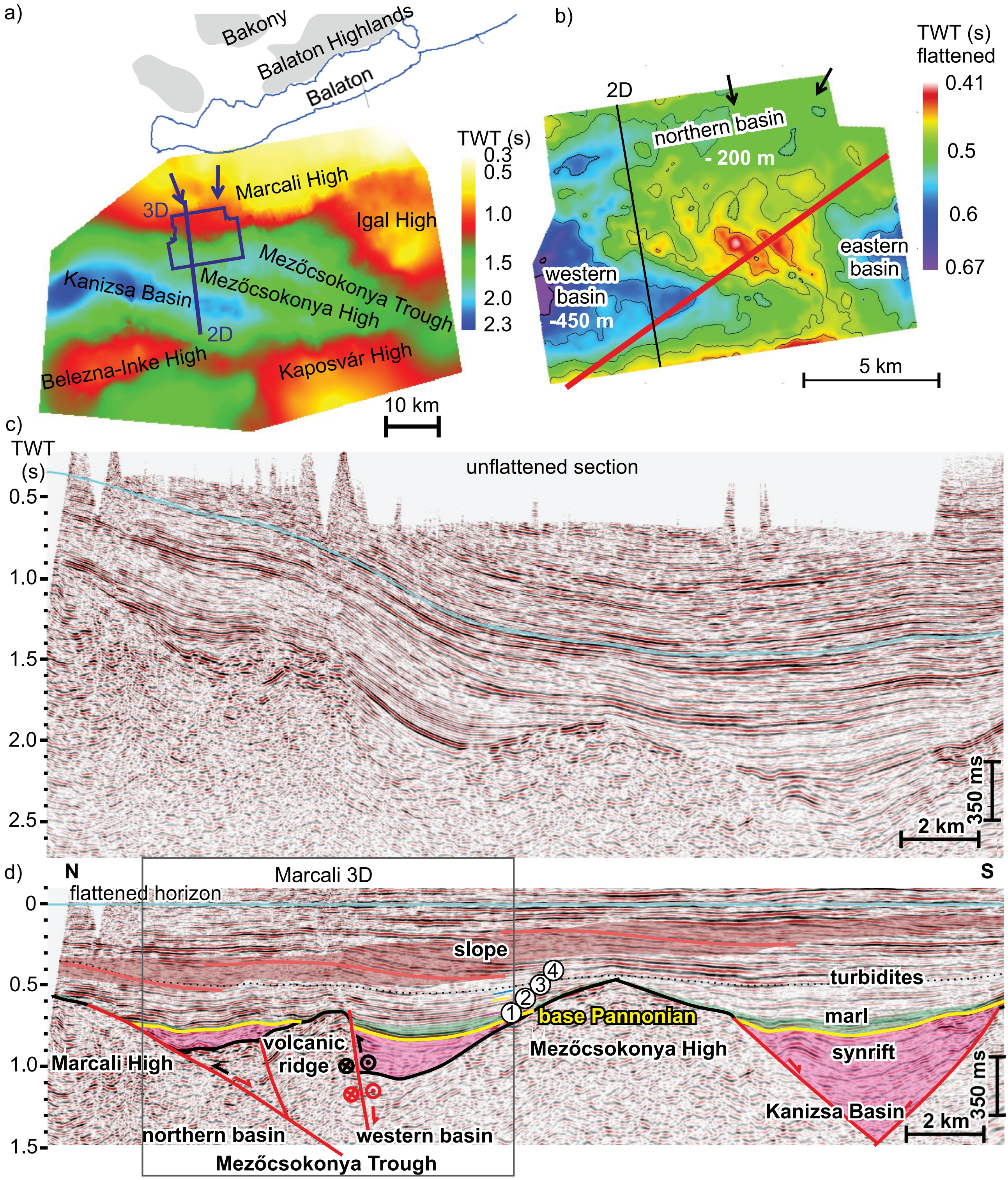

Fig. 7. **(a)** Present day base Pannonian topography of the Kanizsa Basin and Mezőcsokonya Trough (Várkonyi 2012). The 3D seismics is located on the northwestern side of the Mezőcsokonya Trough. **(b)** Paleotopography of the Mezőcsokonya 3D: base Pannonian flattened onto the paleohorizontal deltaic plain. The main features are a shallow northern basin (~200 m), and a deeper western and an eastern basin (~400 m), separated by a volcanic ridge in the middle (0 m). **(c)** Original and **(d)** flattened, interpreted seismic section through the 3D and continued towards the Kanizsa Basin. The Lake Pannon basin floor was very rough on the northern side of the Mezőcsokonya paleohigh and an even floor occurred in the Kanizsa Basin. The topographic differences between the N and S were much less than today, even though a bit more depth than depicted is expected in the S if compaction is taken into account.

(Várkonyi 2012). Beneath the 'northern' basin a Middle Miocene syn-rift basin fill is present, the subsided relief of which was inherited in the Pannonian (Fig. 7). The 'western' basin developed in the Early-Middle Miocene, the escarpment is a sinistral strike-slip fault with a normal component (Várkonyi 2012).

Understanding the structural characteristics of the area is essential for separating the structural and sedimentary features. However, their differentiation still proves difficult since the structural features play a prominent role in sedimentation.

Sedimentary units

Four units can be differentiated, corresponding to four phases in the development of the deep-water system (Figs. 8, 9A).

Unit 1 – marl

The laterally continuous high amplitude seismic facies is characteristic for the Endrőd Marl. It is very thin, 20–70 m thick in the area (Fig. 9A, B), corresponding to 1–2 reflections. Some reflections onlap towards the NNE in the northern and western basin as well and are thin (20 m) on the volcanic ridge.

Unit 2 – basin-floor turbidites

Unit 2 and 3 were mapped in sandy successions belonging to the turbidite-bearing Szolnok Formation (Figs. 8, 9A). The onlapping laterally continuous high amplitude facies is thicker in the downstream western and eastern basins than in the upstream northern basin, while the reflections are thicker in the upstream northern basin than in the lower ones. The unit pinches out on the ridge. Some reflections pinch out where a lower smaller reflection is present.

The spectral decomposition of the basal horizon (2. base) shows several channels (Fig. 8): (a) a channel running towards the SW, avoiding the ridge and going towards the western basin, (b) a sinuous channel with overlapping routes running towards the S, going towards the eastern basin, and (c) channels parallel to the volcanic ridge. The horizon lies approximately 30–100 m above the ridge (Fig. 9A). The cross section of channel c shows that Unit 2 has a set of eastward inclined short, shingled reflectors (Fig. 9B). This transitions towards the E into a thick reflection that is a 60 m thick blocky sand in the well N-6; which thins, possibly pinches out or transitions into two upward fining sand units in well N-3 and a serrated sandy unit in well N-1. Eastward onlaps are present above the volcanic ridges.

The topmost horizon of unit 2 (2. top) has low sinuosity channels, one of the synforms guides a straight channel (Fig. 8d), but the channels cut across the western synform (Fig. 8d, e), as opposed to those of horizon '2. base'.

In the area of the western and the eastern basin, both basal and topmost horizons are smooth, show only faint and short channel-forms and have no internal reflection terminations (Fig. 9A). The reflections between the two horizons pinch out on the volcanic ridge.

Unit 3 – toe-of-slope turbidites

This is a discontinuous variable amplitude seismic facies in the upstream northern subbasin (3a) and a moderately continuous facies with rare channel-forms in the downstream western and eastern subbasins (3b). The reflections drape the ridge, but a few onlaps are still present, e.g the 3a mid and 3b mid reflections both pinch out towards the ridge (Fig. 8). Gently inclined reflections at the northeastern part show the arrival of the toe-of-slope sediments. Downlaps of mound-like reflections and onlaps onto the inclined reflections are common (Fig. 9C), e.g. the northeastern part of horizon 3a base (Fig. 8) is missing due to downlap.

The sinuous channels approach the ridge parallel to its strike based on the spectral decomposition of the basal horizon of unit 3a (Fig. 8f). The basal horizon of unit 3b reveals channels coming from the saddle between the northern and western basins (Fig. 8g), a lobe-like feature, and sinuous channels on top of it in the western basin, going towards the SW or S. One of the sinuous channels is 300 m across and apparently 25 ms thick in TWT (~50 m; Fig. 8D).

Unit 4 – slope

This unit comprises continuous clinoforms (Fig. 9A) with channel-forms in dip view and low amplitude discontinuous facies in strike view. Onlaps and downlaps are common within the unit.

The paleotopography is relatively even. The toe-of-slope channels are well defined on the spectral decomposition map and change their sinuosity during their course, they are the least sinuous near the ridge, and the most sinuous in the western basin. The channels are still diverted near the ridge (Fig. 8). One of the channels (Fig. 8h), cutting through the ridge on its southeastern end, has asymmetric bends: the bends are wider and longer on the dipping western side compared to its higher eastern side.

Interpretation

Unit 1 – marl

Since the Endrőd Marl is exceptionally thin, and the first turbidity currents arrived at a gently south-southwest dipping northern basin, the flows gained momentum and created not only lobes, as common elsewhere, but also channels.

Unit 2 – basin-floor turbidites

There are several reflections that are only present in the western basin, suggesting that the turbidity currents bypassed the upper, northern basin. It is also possible that flow stripping

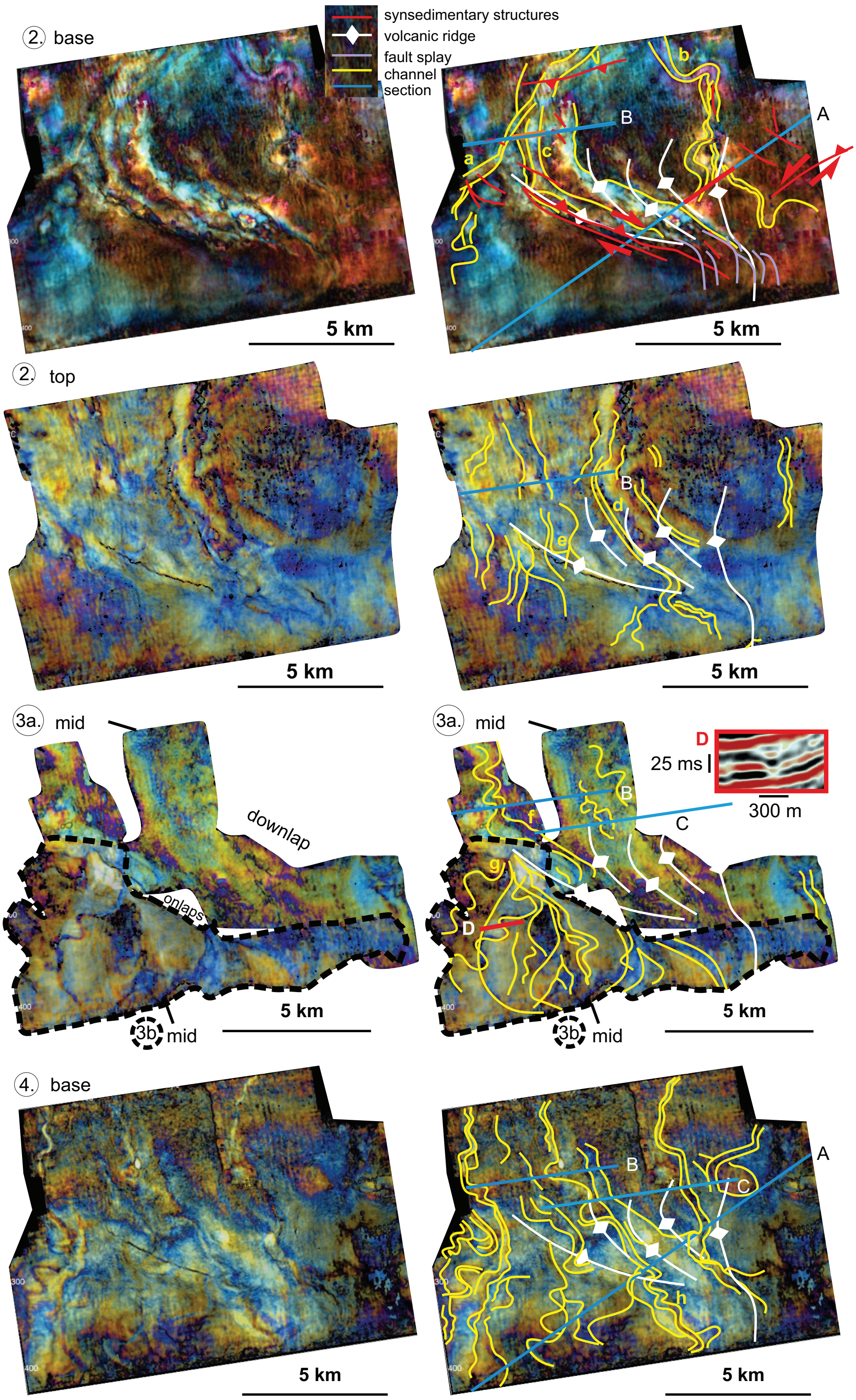

Fig. 8. Spectral decomposition of major stratigraphic units (R: 20 Hz, G: 40 Hz, B: 55 Hz, ±18 ms). Capital letters indicate sections of Fig. 9; lower case letters indicate channels. 2. base: basal horizon of unit 2, that is present in all basins, showing channels avoiding the volcanic ridges and running in the synforms between the ridges. 2. top: topmost horizon of unit 2, where channels are deflected but cross the ridge. 3a. base: basal horizon of unit 3 only present in the northern and eastern basins, channels run parallel to the ridge. 3b. base: basal horizon of unit 3, only present in the western basin, showing a lobate form with sinuous channels feeding it. 4. base: Basal horizon of unit 4, at the gently inclined toe-of-slope, some channels are still diverted, but some cut through the ridge, even though the top of the volcanic ridge is 150–200 m below this horizon.

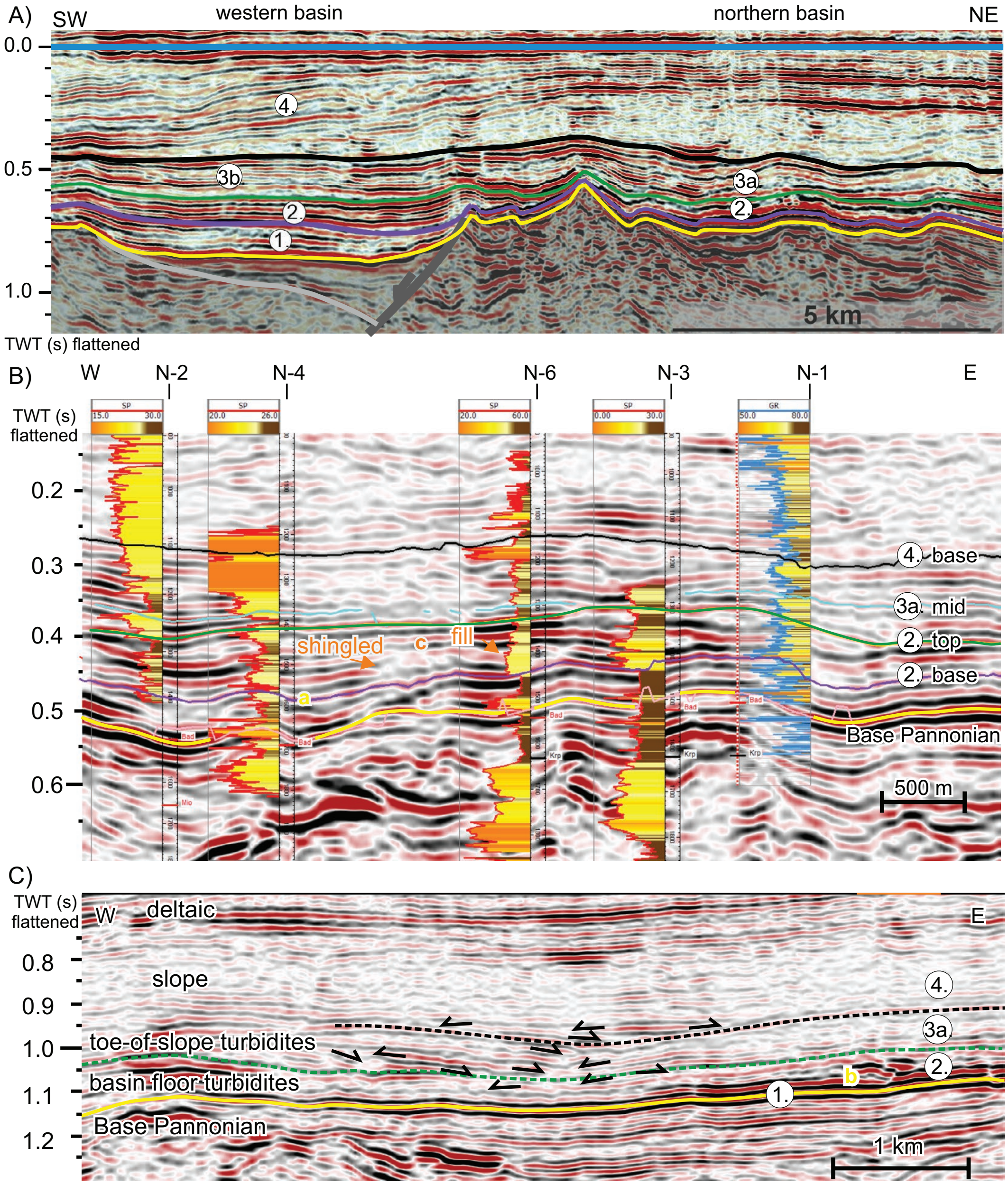

Fig. 9. (A) Sedimentary units on a flattened seismic section that goes through the western basin, the volcanic ridge and the transition between the northern and eastern basin. **(B)** Section through several wells near the top of the volcanic ridge. Well logs are separately facies shaded according to their interpreted shale/sand line, sand – yellow, shale – brown; SP – red curve, GR – blue curve. The channel-form features on the seismic section correspond to blocky or upward coarsening then fining sandy units. Shingled reflectors and thick pinching out reflectors of channel c (Fig. 8) correspond to a blocky sand: the final fill of a channel after a series of lateral migration. **(C)** Onlaps, downlaps, mound-like features in unit 3a and 4 in the northern basin: Compensational architecture in the toe-of-slope turbidites. For location, see Fig. 8.

of the upper, finer material of the turbidity current was supplied to the western basin. This is supported by the thinner reflections in the western basin compared to the northern basin. The thick reflections in the northern basin suggest that tabular bedsets developed in front of the confining ridge. The basal horizon clearly shows the influence of the buried volcanic ridge: the channels either avoid it or follow the synforms. Based on the seismic sections, channel ‘a’ heading towards the western basin was older than the other channels. There must have been a change in the supplying slope channel or a thrust activity for such a remarkable change in trajectory.

Channel ‘b’ going towards the eastern basin shows the changes in the slope profile. First, the straight channel is above grade, probably erosional, then becomes highly sinuos, suggesting a step in the profile and at grade channel. The overlapping channels suggest lateral migration and aggradation of a below grade channel. The channel manages to cut through the easternmost antiform and becomes straight, erosional on the slope of the eastern basin.

The short, shingled reflectors of channel ‘c’ (Fig. 9B) suggest a laterally eastward migrating channel which stopped its migration approaching an antiform and developed an aggrading, blocky channel fill. The synform of well N-3 also has a channel fill (Fig. 9B), the fining upward units suggest either lateral migration which is not corroborated with the reflection image, or gradual abandonment of the channel. The thinner beds on the antiforms can be levees or onlapping channel margin sediments. The volcanic ridges steered the turbidity currents and confined their lateral migration.

The channels at the top of the unit (Fig. 8 2. top, d, e) are straight or low sinuosity, their route is quite different from the channels at the base. Channels cut through the westernmost antiform, but the middle antiform determines the route of a straight channel. The lower sinuosity suggests a more above grade profile: the advancing slope could increase the slope angle, or turbidity currents became higher volume, muddier, or denser, thus more efficient (Kneller 2003).

The smooth reflections without internal reflection terminations in the western and eastern basins suggest lobes or sheets. Since the Mezőcsokonya High south of the 3D seismic block was prominent at this time, turbidity currents must have been reflected or deflected from the high. The continuous reflections may indicate ponding, which is feasible for the western basin, but an escape route is possible towards the Kanizsa Basin. The eastern basin is probably connected to the Mezőcsokonya Trough.

Unit 3 – toe-of-slope turbidites

Downlaps, onlaps and mound-like reflections indicate compensational stacking in the northern basin. They compose the toe-of-slope part of clinothems, where a protrusion is formed, probably by a local advancing delta supplying it. The sediments are compensationally stacked: when one mound became too high, the feeding channel switched to a slightly offset location, then switched back, based on the alternating onlaps/downlaps (Deptuck et al. 2008; Straub & Pyles 2012; Pickering et al. 2015). The top of unit 3 is still uneven, the low between two mounds was filled by onlapping sediments. The deposited lobes or mounds confined the successive flows in a gentle manner. The autogenic confinement on the scale of lobes is classified as small-scale confinement.

The horizons in Unit 3 are continuous between the western and eastern basins, showing that they are both filled simultaneously, albeit by several feeding channels coming from the northern basin. The lobe-like feature in the western basin can indeed be a lobe, supplied by channels from the saddle north of the ridge. Its top can be a channel-mouth, ie. a very short channel-lobe transition zone (CLTZ), common in sand-rich systems (Wynn et al. 2002). The channels supplying and cutting through it are very high sinuosity, suggesting a low relief, but still high run-out flows. At this time, the Mezőcsokonya High just south of the 3D seismics is almost covered by turbidites (Fig. 7d). The basin widened by 2 km since the onset of turbidite sedimentation via onlaps. The longer run-out suggested by the channel pattern may have been connected to this widening, but it is also possible that some turbidity currents surmounted the remaining topography and continued their way to the Kanizsa Basin.

Unit 4 – slope

The slope prograded over a relatively even topography, even the Mezőcsokonya High S of the 3D seismics was covered at that phase (Fig. 7d). This means that the medium-scale confinement has been largely healed by the turbidites. Slope progradation is still affected by the basin-scale topography (Uhrin et al. 2009; Törő et al. 2012). However, the channels of the toe-of-slope still preserve the earlier routes: the ridge still guides them and makes them straighter, and the saddle between the northern and western basin is still a prominent source for channels. The channel with asymmetric bends is very similar to that found in the Makó Trough (Sztanó et al. 2013b) and suggests channel development on a slightly SW dipping relief; the NW bends are confined by the margin.

The slope-parallel northern and western subbasins of the Mezőcsokonya Trough had to be filled before turbidity currents could reach the Kanizsa Basin from this direction. The subbasins represent the medium scale confining topography, several km in length and 100 m in depth, within the basin-scale Mezőcsokonya Trough. The continued effect of basal volcanic topography, long after being buried suggests that structural deformation was still ongoing. The main strike-slip acted as a reverse fault during deposition, preserving some of the relief between the northern and western subbasins. The antiforms and synforms of the volcanic ridge guided the channels even when the Mezőcsokonya Trough was healed. The well logs show that channel sands were prominent in the synforms, but muddy intervals were also present. Differential compaction of muddy sediments above the volcanic ridge could preserve some topography. However, active folds connected to the strike-slip and its splay faults are suggested.

Evolution on a complex slope, Drava: medium- and small-scale confinement

Paleotopography and structural control

The other studied 3D seismic cube is located near the 130 km long NW–SE trending Drava Basin, in its middle region (Fig. 4). The Drava Basin itself is further to the southwest with an aspect ratio of 0.3 (Fig. 2a). The 3D seismic block is on a plateau on its NE flank that provides sediment to the Drava Basin in an oblique angle, the slope progradation is not affected by the basin on the Hungarian side. The 3D seismic data cover the southeasternmost end of the Görgeteg–Babócsa High, a plateau extending from the NNW and the margin of the basin towards the Mecsek Mountains.

The current base Pannonian surface (Fig. 4) is similar to the early Pannonian paleotopography (Fig. 10); however, the relief was more irregular in the Pannonian, albeit with smaller depth differences. The structural setting of the area is determined by Cretaceous thrusts and anticlines, which were reactivated during the earliest Pannonian, 11–10 Ma (Oross 2015). At the time of the shelf slope progradation, the extensional phase created several small normal faults; and later negative flower structures and an atectonic polygonal fault system developed (Oross 2015).

Sedimentary units

Five seismic units can be differentiated in the deep-water succession of the area. Unit 1 corresponds to the Endrőd Marl, which is 120–200 m thick and pinches out at the anticline (Fig. 10b). Unit 2 to 4 are part of the basin-floor turbidites Szolnok Formation. Unit 2 has disturbed, but fairly continuous reflections; it is thick in the lows but pinches out towards NE. The four reflections that comprise Unit 3 have high amplitude and are only present in the NE syncline, onlapping in two directions towards the limbs. Unit 4 reflections are continuous and create an evened-out topography. Unit 5 comprises the clinoforms of the Algyő Formation that generally dip towards the S.

H1 horizon is the top of Unit 2, it is located in a small basin (Darány Basin), and it onlaps towards the SW. The spectral decomposition shows several channels (Fig. 11). The channels come from the NNW, channel b has a migrating turn towards the SE and follows the axis of the syncline, before crossing the syncline and the tip of the rotated fault block. Channel 'a' cuts off the bend of channel 'b' in a straight line, but turns E before the tip of the block in a curved bend, then joins channel 'b' before both turn towards the SW. Channel 'c' is of low sinuosity, reaches the area from the NE and apparently joins channels a and b before continuing towards the SW. The well logs show that the onlapping reflections are alternations of 10–30 m thick sandy and muddy units. Correlation inside Unit 2 based on the logs is not evident, A is sandier than well B and intervals have slightly different characters. The amplitude of seismic reflections decreases or increases intermittently, in a width of 150–300 m, corresponding to channel forms on the spectral decomposition.

H2 Horizon of Unit 3 corresponds to a roughly evened out relief just below the slope clinoforms. The channels follow the relief: they are NW–SE oriented and are high sinuosity, except above the Görgeteg–Babócsa High where they are straight. Lateral migration is not observable, but overlapping routes occur. In the NE, the southward going channel 'd' still turns towards the strike of the previous syncline in a straight manner, but it is offset towards its limb. The turn of the channel towards the southern trough is (approximately at the same position as in the case of H1 Horizon, before that, highly sinuous bends occur.

Facies analysis of the core

Well A has a 45 m core, and a suite of well logs (Fig. 12a). The core starts 60 m above the top of Endrőd Formation, and includes two major sand bodies, separated by shale (Fig. 12b). There are seven smaller units in the core, within the two major sand bodies, of which five are ~5 m thick upward coarsening and two are ~10 m thick upward fining units.

The cores can be divided into 6 facies: (F1) structureless ungraded sandstones, some banded (Fig. 12c); (F2) graded sandstones with loading, water-escape structures, mud clasts (Fig. 12d, e, f, g); (F3) chaotic muddy sandstone with mud clasts (Fig. 12h, i); (F4) parallel and cross-laminated sandstones, climbing-ripple cross lamination, convolution in places, up to 1.5 m thick (Fig. 12d, j); (F5) siltstone with plant debris, bedded-laminated; and (F6) homogenous clayey silt.

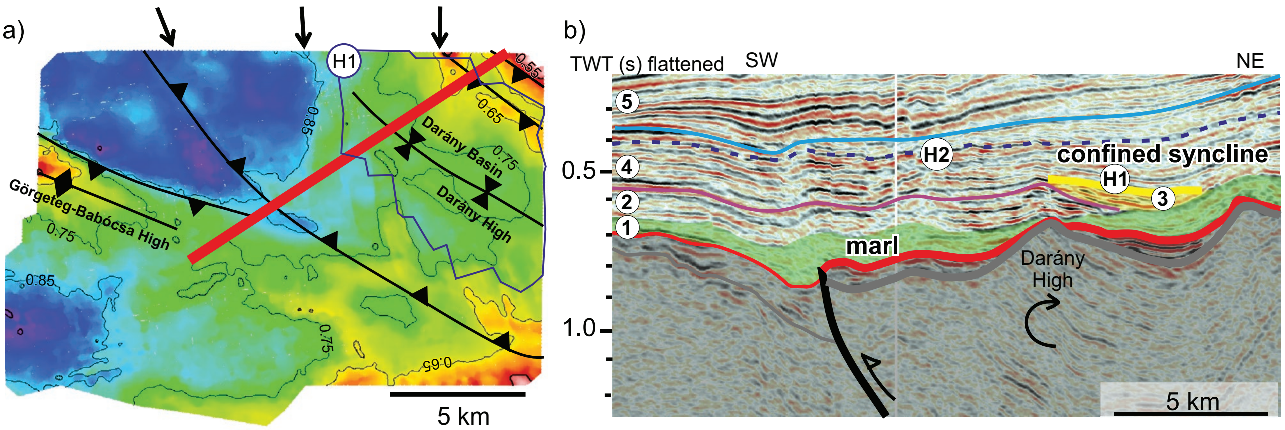

Fig. 10. (a) Flattened paleotopography of the base Pannonian on the Drava Basin 3D data (Fig. 4 – B, TWT, s), showing the anticlines, synclines and thrusts that shaped the Pannonian relief, sediment input direction is N-to-S. **(b)** Flattened seismic section showing a series of anticlines and synclines related to the earlier and synsedimentary folding. The latter occurred due to block rotation on the thrust fault. H1 horizon and the lenticular body below it show two-way onlapping. H2 horizon and the first toe-of-slope downlapping horizon (blue) were deposited on a relatively even relief.

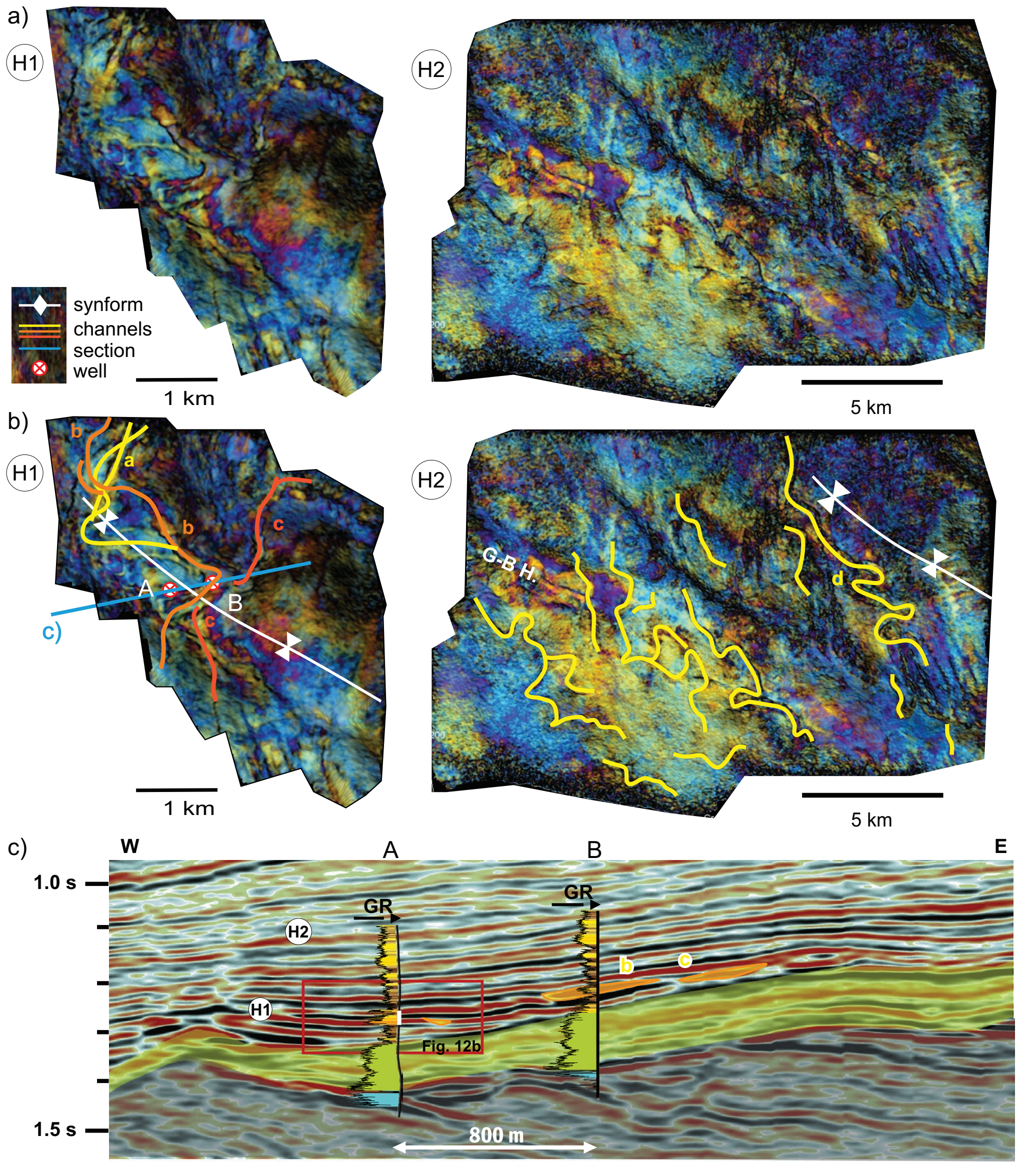

Fig. 11. (a) Uninterpreted and **(b)** interpreted spectral decomposition (R: 20 Hz, G: 40 Hz, B: 50 Hz, ±18 ms) of H1 and H2 horizons. The H1 horizon is only present in the NE part of the seismic, NE of the anticline, location on Fig. 10a. **(c)** Seismic section with well logs (GR: gamma ray) in the NE syncline, showing the channel fills of H1 horizon. G-B H.: Görgeteg–Babócsa High.

The facies are interpreted as follows: (F1) sandstones were formed by aggradation beneath high-density turbidity currents (Kneller & Branney 1995), banding might be the result of weakened turbulence from dispersed clay (Haughton et al. 2009). (F2) sandstones are the result of aggradation beneath non-cohesive high-density turbidity currents (Kneller & Branney 1995; Talling et al. 2012). (F3) muddy sandstones must be cohesive debris flow deposits (Haughton et al. 2009). (F4) structured sandstones are produced by traction sedimentation by dilute flow, the thick intervals by sustained pulsing flows (Kneller & Branney 1995; Talling et al. 2012). (F5) siltstone was deposited by suspension fallout with shearing. (F6) clayey silt was created by suspension fallout without shearing and possible subsequent bioturbation.

No thick mud cap was observed, supporting that currents were not fully ponded in the syncline. Beds of structureless or banded sandstones capped by chaotic muddy sandstones with mud clasts and laminated intervals may be the products of hybrid events. Only a few of these full beds are present, but chaotic muddy sandstones are common.

The lower sand body has more thick structured sandstones (F4), while the upper unit has more rip-up mudclasts. At the core location, no channel-form can be observed on the seismic; however, there are decreased amplitudes 100–200 m away from the well, corresponding to channel-forms on the spectral decomposition. The channel fills are 100 to 500 m wide and 20 to 30 m thick. The well correlation shows that well A is sandier and sandbodies are thicker than in well B (Fig. 11c).

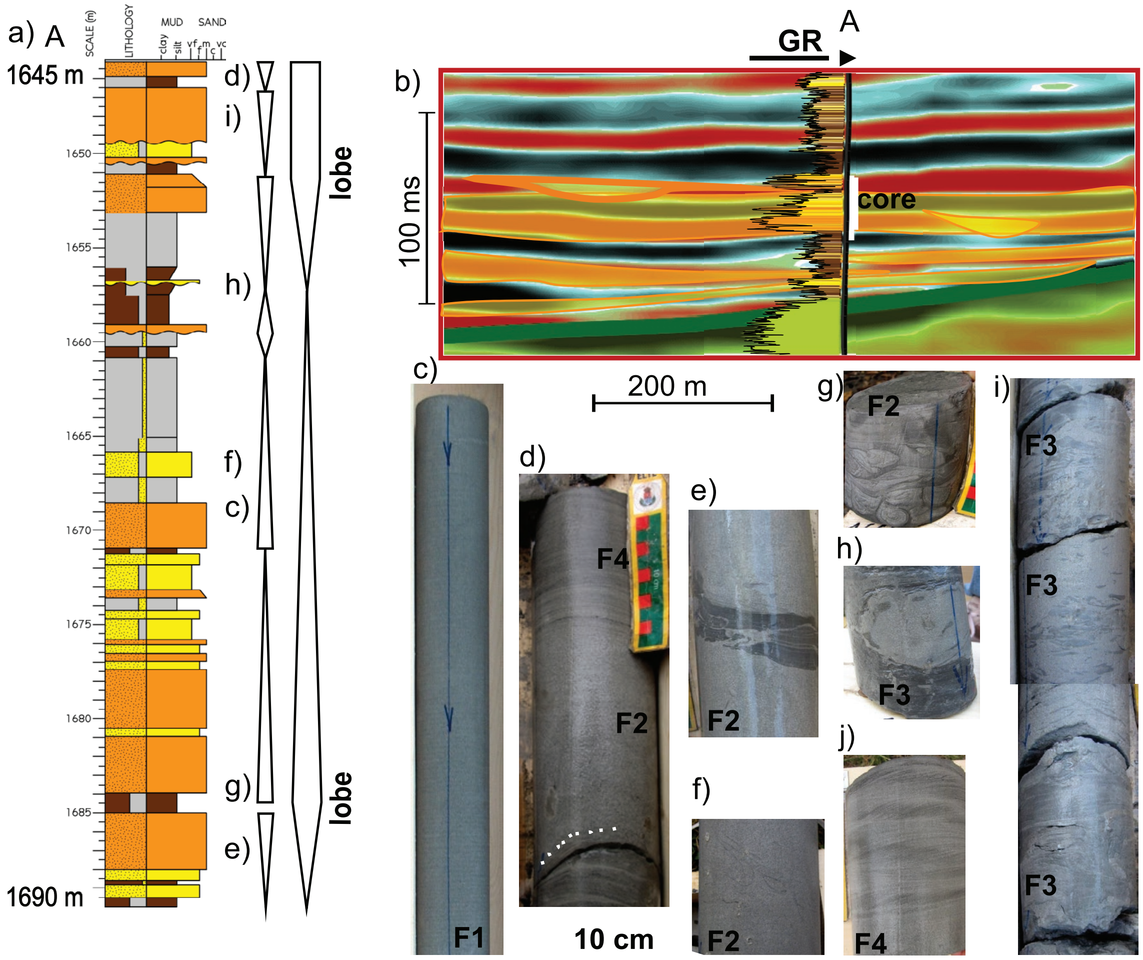

Fig. 12. **(a)** Sedimentary log of the cored interval of well A (Fig. 11b, c); **(b)** seismic interpretation of channels and lobes in the vicinity, gamma ray log in cored well. Common facies of the core: **(c)** structureless sandstone (F1); **(d)** small flames on bottom of graded, structureless (F2) to laminated (F4) turbidite bed; **(e)** rip-up mud-clasts in medium-grained structureless sandstone (F2); **(f)** faint water-escape pipes in medium-grained sandstone (F2); **(g)** well-developed load structures: balls and flames (F2); **(h)** chaotic, deformed massive medium-grained sandstone and rip-up clay-clasts, burrows penetrate to underlying siltstone (F3); **(i)** rip-up mud-clasts of varying size in chaotic sandstone (F3); **(j)** well-developed climbing-ripple cross-lamination (F4).

Interpretation

The approximate paleotopography of Lake Pannon just before turbidite deposition shows that thrusts and related folds shaped the topography. Hemipelagic marl was covered by sheet-form turbidites. The synsedimentary reactivation of a thrust and induced block rotation caused the development of a confined syncline (Darány Basin) upstream of the main trough.

The metre-scale coarsening and fining upward units of the core are interpreted as lobe elements that make up the two 15 and 30 m thick lobes. The frequent high-density currents, water escape, loading and thick structured sandstone deposition points to a high energy environment. In addition, channel architectural elements are close by, suggesting channelised lobes. Ponding may have not taken place at this point, based on the lack of thick mudcaps. However, ponding cannot be ruled out earlier, during the deposition of the first 50 m of the fill. The continuous, high amplitude reflector, the low net-to-gross in wells may be a result of the ponding; and the narrow bowl shape of the basin could prevent sand from escaping. However, the energetic nature of the successive channels shows that the flows could easily surmount the topography.

Hybrid events may be related to flow reflection, but also a range of flow transformations, e.g. on frontal lobe fringes, or at channel-levee transition zones (Patacci et al. 2014; Spychala et al. 2017a; Fonnesu et al. 2018; Brooks et al. 2022). Here, the confinement or the turbulent erosion in channels may be responsible for hybrid events.

The channels met the syncline perpendicularly, in a frontally confined scenario, trending first towards the base of the confined syncline (H1, a), then were deflected at the limb of the syncline and followed its strike (H1, b). Onlaps on both limbs of the syncline suggest a lateral confinement from this point on. However, the channels found a way towards the lower sub-basin, eroding the barrier (H1, c). The net-to-gross is the larger near the tip of the rotated block (Well A; Fig. 12), where the upper, muddier part of the flows might spill laterally into the lower trough. The channelized lobe setting, based on the core and seismics, can be regarded as an intraslope lobe.

After the initial confinement was reduced (H2), the basin topography was largely filled, but the main troughs and highs still guided the channels towards the SE, even though the slope supplied the turbidity currents from the N. Slight block rotation could still straighten the NE channel above the syncline and a flat step in the slope profile or a slight confining tilt could induce the sudden change to high sinuosity. The few channels that cut through the Görgeteg–Babócsa High became straight on top of it, suggesting that they were erosional. The general high sinuosity and lack of lateral migration means that the channels were slightly below grade and were aggrading. Avulsion took place, leading to overlapping channels. The lateral migration of channels in the confined syncline, the erosional channels and the aggrading channels all confined the successive turbidity currents (Brunt et al. 2013), this can be regarded as the small-scale confinement.

Discussion

Three scales of confinement can be inferred in the Pannonian Basin System, based on the dimensions and genetics of basins, style and spatial prevalence of confinement and evolution of the sedimentary system: basin-scale, medium-scale and small-scale confinement. Basin-scale confinement constitutes the large depressions of the Pannonian Basin System. The dimensions of basins vary greatly, but a 20–140 km length or width, >50 km^2 area and minimum 200 m, but generally >500 m confining height is proposed for their classification. The Zala Basin constitutes a basin-scale depression, the Belezna Anticline represents its frontal margin. It is segmented by frontally confining highs where flow stripping created sandy depocentres. Turbidity currents could partly surmount or flow around the Budafa, Kilimán Highs and the noses, so these ridges are rather a part of the medium-scale confinement.

The medium-scale confinement corresponds to smaller individual basins and subbasins nested into the large depressions. They are best described by 2–20 km length or width, 30–100 km^2 area; and 50–400 m depth. They are much closer in scale to the dimensions of the architectural elements: channels are generally 200–1000 m wide, lobes are 4–100 km^2 in the toe-of-slope region (Sztanó et al. 2013b). The Mezőcsokonya Basin represents basin-scale confinement, its subbasins: the northern and western basins are medium-scale features. The basin-scale Drava Basin has also medium-scale depressions: the Darány Basin and the troughs on either side of the Görgeteg–Babócsa High. These medium-scale basins are in the range of the Gulf of Mexico salt-withdrawal minibasins (Prather et al. 1998), Karoo Basin intraslope minibasins (Spychala et al. 2015), and the smaller basins of the Annot Sandstones (Smith & Joseph 2004).

The small-scale confinement represents the depositional topography on the scale of architectural elements. It can be captured regarding the autogenic compensational stacking of lobes, e.g. in the eastern basin of Mezőcsokonya, and the high energy environment of channels that confine flows laterally (Tőkés et al. 2021), e.g. straight, erosional channels, and laterally migrating channels of the 3D blocks.

There are similarities between the basin-scale confinement and medium-scale confinement in the Pannonian Basin (Fig. 13):

- Both scales of confinement lead to sand depocentres near lateral margins when there is a rugosity of the floor (on the scale of 1–40 km in wavelength, and 50–400 m in depth), and on the upstream side of basement highs. The deposits are frequently thicker than the rest of the area.
- Both scales of confinement lead to onlaps onto the basin floor, i.e. sandy pinch-outs that are viable stratigraphic traps.
- Flow transformation into hybrid events, probably related to confinement, has been documented on both scales: Želiezovce Basin (Vlček et al. 2024; Šujan et al. 2025), Makó Trough (Sztanó et al. 2026) on the basin-scale, Darány syncline of Drava on the medium-scale (Fig. 11).
- Reflection induced sheet deposition is prevalent in the basin-scale confined setting: continuous reflections and tabular lobes based on well logs in the Makó Trough (Sztanó

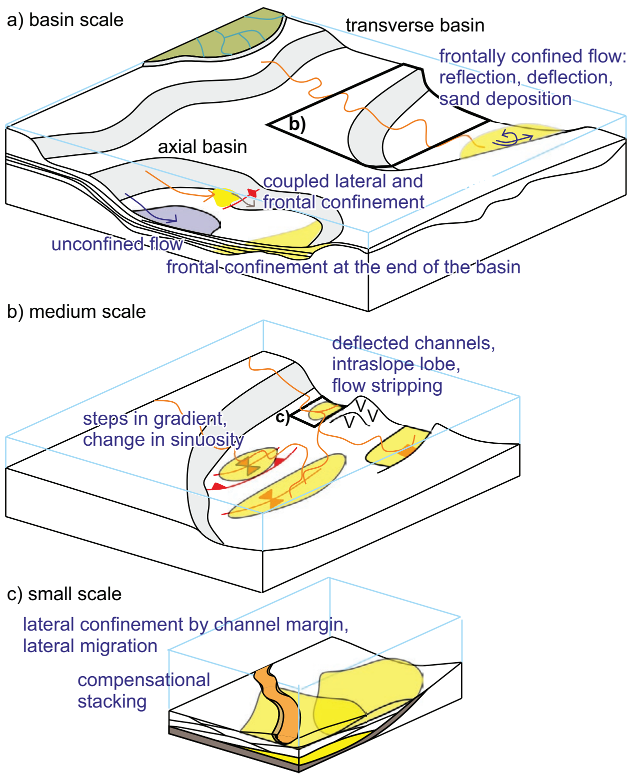

Fig. 13. Scales of confinement in the Pannonian Basin.

et al. 2013b) and downstream part of the Mezőcsokonya Basin (Fig. 6); but can also be found in the western and eastern medium-scale basins.

There are also a few differences between the two scales:

- Flow stripping, i.e. retention of sand in the upstream basin and muddy overspill into the downstream basin, is a feature in medium-scale confinement, based on net-to-gross and reflection thickness relations. The basin-scale frontal margins are generally too high to surmount.
- Medium-scale confinement is generally healed before the prograding toe-of-slope arrives; however, the first toe-of-slope channels and lobes are still somewhat guided by the underlying relief. Basin-scale confinement is generally not healed before the slope arrives and it significantly affects the slope progradation.
- Medium-scale confinement is present on the upstream slopes of large-scale basins, creating a lengthened, topographically complex slope with deflected channels, intraslope lobes, changing sinuosity of channels (Brooks et al. 2018). Basin-scale confinement provides the dip of upstream slopes but does not create the complexity.
- In the case of large basins where medium-scale confining ridges are lacking or are already healed, channels and lobes can develop in an unconfined manner on the basin floor without reaching the margins. The basin-scale confinement may only be significant near the lateral and frontal margins and not on the basin plain. In contrast, medium-scale confinement has an effect on all flows meeting it.
- Medium-scale confinement is controlled by factors in this order of importance: synsedimentary deformation, presedimentary deformation, differential compaction, volcanic ridges. In contrast, basin-scale confinement is controlled by factors in this order of importance: presedimentary deformation, synsedimentary deformation.

The small-scale confinement primarily develops on unconfined basin floors at the basin scale, or on healed topography at the medium scale. Compensational stacking did not develop in possible ponded or strongly reflected scenarios, because there, the confinement created tabular bedsets on seismic scale. It only occurs on steps where there are escape routes, and they are related to the irregular progradation of the toe-of-slope.

The processes related to flow confinement, such as flow deceleration, deflection, reflection, decoupling, stripping, transformation, ponding, are similar across scales, but their stratigraphic expression and significance changes with scale. The different topographic wavelengths of the two scales, nested within the other, are met with similar currents, but on different parts of their pathway: they provide complex slope profiles or abruptly ended, confined slope profiles (Kneller 2003). The style of confinement is also controlled by the basin shape, the angle of incidence, the amplitude of the relief, and the spatial continuity and sill efficiency of the topography. The original amplitude of the relief, together with syndepositional deformation and compaction, controls the persistence of relief through time, thus the rate of healing by sedimentation (Felletti & Bersezio 2010; Prather et al. 2012; Nyíri et al. 2021). The dimensional limits of the scales depend on the characteristic dimensions and runout potential of average and the largest, outsized turbidity currents inhabiting a given system. The dimensions of unconfined depositional elements, such as channel fills, channel complexes, lobe elements and lobe complexes (Cullis et al. 2018), provide a reference scale against which the size of topographic obstacles can be evaluated. The major difference between basin- and medium-scale confinement is the persistence of relief, and the possibility for unconfined deposition on basin floors away from basin-scale margins. Since basin dimensions and morphologic complexities form a continuum, and many confinement-related processes recur across scales, the distinction between basin-scale and medium-scale confinement is primarily based on the persistence, spatial extent and stratigraphic influence of the confining topography.

The proposed scales of confinement are also relevant for hydrocarbon exploration. Basin-scale structural highs not only form potential traps during later tectonic evolution but also precondition the location of sand accumulation, thus the excellent reservoir quality and pinch-out geometry. The apparent 4–10 km upstream offset of sand depocentres relative to ridge axes further suggests that the angle of incidence between turbidity currents and basin margins should be considered when predicting frontally confined sand depocentres. Smaller structural features of medium-scale confinement, hidden under healed topography, should also be targeted, as they can efficiently retain sand on steps of slopes and silled subbasins (Smith 2004; Brooks et al. 2018).

The routes, sinuosity and fill of channels should be mapped on 3D seismics on all scales. These features also help us in determining the topographical relations and slope profiles not always discernible from stratigraphic surfaces. Since both the Mezőcsokonya and Drava examples are on the upstream ends of larger basins, the margins act as slopes for the incoming turbidity currents. Due to their pre-, synsedimentary, volcanic and compactional topography, they are not simple, or stepped slope profiles, but topographically complex ones. Obstacles are avoided, channels get deflected at frontal or oblique confining ridges, and spill points develop at the end or middle of the confining ridge; similar to other confined examples (Fugelli & Olsen 2007; Dmitrieva et al. 2018; Dodd et al. 2019). Steps in the slope profile, e.g. by a minibasin or a terrace, increase the sinuosity of channels and favour sand deposition on intraslope lobes (Brooks et al. 2018). Where confining ridges create narrow corridors, straight channels develop. At spill points, upon entering a lower basin with steeper slopes, the channels become straight and incisional and increase their sinuosity on the basin plain.

The confinement hierarchy recognized in the Pannonian Basin System demonstrates that inherited and syndepositional topography controlled sediment routing, sand distribution and depositional architecture across multiple spatial scales. Similar interactions between nested confinement, slope complexity and topographic healing have been described from other confined deep-water systems, including salt-withdrawal mini-basins (Prather et al. 2012; Oluboyo et al. 2014), convergent margin (Bourget et al. 2011) and the Karoo Basin (Spychala et al. 2015; Brooks et al. 2018). The proposed subdivision into basin-, medium- and small-scale confinement therefore provides a practical framework for interpreting structurally complex deep-marine systems and predicting reservoir distribution in confined basins. The proposed quantitative limits between scales are a first approximation for the Pannonian Basin System and require further testing, in other basins and datasets as well.

Conclusions

This study demonstrates that turbidite confinement in the Pannonian Basin System operated as a hierarchical, nested system of topographic controls acting at three scales: basin-scale, medium-scale and small-scale confinement (Fig. 13). Although similar confinement-related processes recur across scales, including flow deflection, reflection, stripping, ponding and transformation, their spatial extent, persistence and stratigraphic expression differ sufficiently to justify their distinction.

The most obvious external controls on turbidite confinement are the basin area, the aspect ratio and the incidence angle of the turbidity currents or slope progradation (cf. Sztanó et al. 2026). These simple characteristics provide a way for comparing basins within the Pannonian Basin System and finding worldwide analogues. If the volume, density, sand:mud ratio of turbidity currents is similar, the degree of confinement should be similar in basins with the same characteristics. The Pannonian basins are in the range of medium to larger confined basins of the literature and constitute the large-scale, i.e. basin-scale confinement of the Pannonian Basin System.

Basin-scale confinement was controlled primarily by inherited and syndepositional structural depressions and highs. These large-scale topographic elements governed the overall sediment-routing pathways, the distribution of depocentres and the location of preferential sand accumulation.

Sandy depocentres in the Zala area are linked to frontal structural highs. High frontal margins – Belezna Anticline, southern ends of the Mezőcsokonya and Ozora Troughs – promoted sandy depocentres, stratigraphic pinchouts, and sandy, tabular lobe elements to lobe compexes continuous over 1–2 km. Aggradational onlaps developed on low gradient slopes, scattered onlaps developed on steeper frontally confining slopes, probably due to varied reflection, deflection, and deceleration responses to the strong confinement.

Lateral confinement alone did not develop sandy depocentres. A rugosity of the basin floor – indentation of the margin, due to anticlines, reverse faults, or other structures – was essential in facilitating sand deposition. This rugosity constitutes as medium-scale confinement, was around 50–200 m in slope height, and created sandy depocentres of 5–10 km areal extent.

Incipient, or growing, gentle antiforms or any other ridges perpendicular to flow have produced onlapping thick turbidites, sandy depocentres upstream of them and thinner turbidite units downstream of them, probably owing to reflection, deflection or deceleration of sandy flows, and flow stripping of the finer upper parts of currents downstream.

Medium-scale confinement was generated mainly by syndepositional deformation, locally enhanced by volcanic topography, inherited structures and differential compaction. Generally, such basins are 2–20 km in length or width, 30–100 km^2 in area; and 50–400 m in depth. These features created complex slope profiles, silled subbasins and local topographic barriers that controlled channel routing, erosion and deposition. In both the Mezőcsokonya and Drava examples, channels were deflected around obstacles, confined within intraslope basins, creating high net-to-gross channel fills or channelized lobes, resulting in predictable sand accumulation patterns. Medium-scale relief was commonly healed before the arrival of the fully developed shelf-margin slope, although buried structures continued to influence channel pathways.

Small-scale confinement operated at the scale of individual architectural elements, including channels and lobes. Here, depositional topography controlled compensational stacking of toe-of-slope lobes, channel migration and the routing of subsequent flows. Unlike basin- and medium-scale confinement, it represents an autogenic component of system evolution.

The results indicate that confinement in the Pannonian Basin System is better described as hierarchical rather than fractal-like. Similar processes occur across scales, but the scales themselves are distinguished by the persistence of relief, the proportion of flows affected and the resulting stratigraphic architecture. Basin-scale confinement may allow largely unconfined deposition across basin floors while strongly influencing basin margins, whereas medium-scale confinement affects nearly all flows encountering the obstacle.

The quantitative thresholds proposed here represent a first-order framework for the Pannonian Basin System rather than universally applicable limits. Confinement scales likely emerge from the interaction between turbidity-current magnitude and topographic relief, forming a continuum of influence rather than discrete categories. Nevertheless, the hierarchical subdivision provides a useful framework for interpreting sediment routing, depositional architecture and reservoir distribution in structurally complex deep-water systems.

From an exploration perspective, basin- and medium-scale topography should be considered key predictors of reservoir presence and quality because they strongly influence the location of sand accumulation and subsequent trap development.

Acknowledgements: This study has been part of Lilla Tőkés's PhD Thesis. We are grateful for the reviewers of this paper, András Uhrin and Marco Patacci for their thorough suggestions. Reviewers of the PhD thesis: Zoltán Sylvester and Dejan Radivojević are thanked for their constructive criticism that greatly improved the base of this paper. We are grateful for the data provided by HHE North Ltd. and Magyar Horizont Energia Ltd. András Uhrin is sincerely thanked for providing digital grids of the Fodor et al. (2013) paper. The study was supported by Hungarian National Research, Development and Innovation Office (NKFIH) projects no. 116618 and 143787. Academic licences were kindly provided to ELTE by SandP Global (IHS-Kingdom) and dGB Earth Sciences (OpendTect).

References

Amy L.A. & Talling P.J. 2006: Anatomy of turbidites and linked debrites based on long distance (120×30 km) bed correlation, Marnoso Arenacea Formation, Northern Apennines, Italy. *Sedimentology* 53, 161–212. https://doi.org/10.1111/j.1365-3091.2005.00756.x

Amy L.A., McCaffrey W.D. & Kneller B.C. 2004: The influence of a lateral basin-slope on the depositional patterns of natural and experimental turbidity currents. *Geological Society, London, Special Publications* 221, 311–330. https://doi.org/10.1144/GSL.SP.2004.221.01.17

Árgyelán G.B., Zadravecz Cs., Nyiri D. & Magyar I. 2026: Seismic stratigraphic units, palaeogeography and their effect on hydrocarbon distribution in the upper Neogene of the Pannonian Basin. *Geological Society, London, Special Publications* 554, SP554-2024–52. https://doi.org/10.1144/SP554-2024-52

Balázs A., Matenco L., Magyar I., Horváth F. & Cloetingh S. 2016: The link between tectonics and sedimentation in back-arc basins: New genetic constraints from the analysis of the Pannonian Basin. *Tectonics* 35, 1526–1559. https://doi.org/10.1002/2015TC004109

Balázs A., Granjeon D., Matenco L., Sztanó O. & Cloetingh S. 2017: Tectonic and Climatic Controls on Asymmetric Half-Graben Sedimentation: Inferences From 3-D Numerical Modeling. *Tectonics* 36, 2123–2141. https://doi.org/10.1002/2017TC004647

Balázs A., Magyar I., Matenco L., Sztanó O., Tőkés L. & Horváth F. 2018: Morphology of a large paleo-lake: Analysis of compaction in the Miocene-Quaternary Pannonian Basin. *Global and Planetary Change* 171, 134–147. https://doi.org/10.1016/j.gloplacha.2017.10.012

Balázs A., Oravecz É., Bartha A., Fodor L., Magyar I. & Sztanó O. 2026: Tectonostratigraphic models of an extensional back-arc basin: inferences for the evolution of the Pannonian Basin System. *Geological Society, London, Special Publications* 554, SP554-2024–83. https://doi.org/10.1144/SP554-2024-83

Berczi I. & Phillips R.L. 1985: Processes and depositional environments within Neogene deltaic-lacustrine sediments, Pannonian Basin, Southeast Hungary. *Geophysical Transactions* 31, 1–3. https://doi.org/10.3133/ofr85360

Bourget J., Zaragosi S., Ellouz-Zimmermann N., Mouchot N., Garlan T., Schneider J.L., Lanfumey V. & Lallemant S. 2011: Turbidite system architecture and sedimentary processes along topographically complex slopes: the Makran convergent margin. *Sedimentology* 58, 376–406. https://doi.org/10.1111/j.1365-3091.2010.01168.x

Brooks H.L., Hodgson D.M., Brunt R.L., Peakall J., Poyatos-Moré M. & Flint S.S. 2018: Disconnected submarine lobes as a record of stepped slope evolution over multiple sea-level cycles. *Geosphere* 14, 1753–1779. https://doi.org/10.1130/GES01618.1

Brooks H.L., Ito M., Zuchuat V., Peakall J. & Hodgson D.M. 2022: Channel-lobe transition zone development in tectonically active settings: Implications for hybrid bed development. *The Depositional Record* 829–868. https://doi.org/10.1002/dep2.180

Brunt R.L., Hodgson D.M., Flint S.S., Pringle J.K., Di Celma C., Prélat A. & Grecula M. 2013: Confined to unconfined: Anatomy of a base of slope succession, Karoo Basin, South Africa. *Marine and Petroleum Geology* 41, 206–221. https://doi.org/10.1016/j.marpetgeo.2012.02.007

Covault J.A., Hubbard S.M., Graham S.A., Hinsch R. & Linzer H.G. 2009: Turbidite-reservoir architecture in complex foredeep-margin and wedge-top depocenters, Tertiary Molasse foreland basin system, Austria. *Marine and Petroleum Geology* 26, 379–396. https://doi.org/10.1016/j.marpetgeo.2008.03.002

Csillag G., Fodor L., Sebe K., Müller P., Ruszkiczay-Rüdiger Zs., Bozsó E.T. & Bada G. 2010: A szélerózió szerepe a Dunántúl negyedidőszaki felszínfejlődésében. *Földtani Közlöny* 140, 463–482.

Csontos L., Dunkl I., Koroknai B., Tari G., Soós B., Magyari Á., Nyíri D., Soták J., Wórum G., Tóth T. & Kovács G. 2026: The formation and deformation of the Neogene Pannonian Basin: a structural overview. *Geological Society, London, Special Publications* 554, SP554-2023–222. https://doi.org/10.1144/SP554-2023-222

Cullis S., Colombera L., Patacci M. & McCaffrey W.D. 2018: Hierarchical classifications of the sedimentary architecture of deep-marine depositional systems. *Earth-Science Reviews* 179, 38–71. https://doi.org/10.1016/j.earscirev.2018.01.016

Deptuck M.E., Piper D.J.W., Savoye B. & Gervais A. 2008: Dimensions and architecture of late Pleistocene submarine lobes off the northern margin of East Corsica. *Sedimentology* 55, 869–898. https://doi.org/10.1111/j.1365-3091.2007.00926.x

Dmitrieva E., Jackson C.A.L., Huuse M. & Kane I.A. 2018: Regional distribution and controls on the development of post-rift turbidite systems: insights from the Paleocene of the eastern North Viking Graben, offshore Norway. *Geological Society, London, Petroleum Geology Conference series* 8, 147–170. https://doi.org/10.1144/PGC8.31

Dodd T.J.H., McCarthy D.J. & Richards P.C. 2019: A depositional model for deep-lacustrine, partially confined, turbidite fans: Early Cretaceous, North Falkland Basin. *Sedimentology* 66, 53–80. https://doi.org/10.1111/sed.12483

Dorrell R.M., Patacci M. & McCaffrey W.D. 2018: Inflation of Ponded, Particulate Laden Density Currents. *Journal of Sedimentary Research* 88, 1276–1282. https://doi.org/doi.org/10.2110/jsr.2018.65

Etienne S., Mulder T., Bez M., Desaubliaux G., Kwasniewski A., Parize O., Dujoncquoy E. & Salles T. 2012: Multiple scale characterization of sand-rich distal lobe deposit variability: Examples from the Annot Sandstones Formation, Eocene–Oligocene, SE France. *Sedimentary Geology* 273–274, 1–18. https://doi.org/10.1016/j.sedgeo.2012.05.003

Falus Gy., Cseresznyés D., Szamosfalvi Á., Szabó-Krausz Zs., Szabó Cs. & Király Cs. 2026: Geological storage of CO_2 in Hungary: the overview of storage potential and the role of natural occurrences. *Geological Society, London, Special Publications* 555, SP555-2023-196. https://doi.org/10.1144/SP555-2023-196

Felletti F. 2002: Complex bedding geometries and facies associations of the turbiditic fill of a confined basin in a transpressive setting (Castagnola Fm., Tertiary Piedmont Basin, NW Italy). *Sedimentology* 49, 645–667. https://doi.org/10.1046/j.1365-3091.2002.00467.x

Felletti F. & Bersezio R. 2010: Quantification of the degree of confinement of a turbidite-filled basin: A statistical approach based on bed thickness distribution. *Marine and Petroleum Geology* 27, 515–532. https://doi.org/10.1016/j.marpetgeo.2009.11.003

Fodor L., Uhrin A., Palotás K., Selmeczi I., Tóthné Makk Á., Riznar I., Trajanova M., Rifelj H., Jelen B., Budai T., Koroknai B., Mozeticc S., Nádor A. & Lapanje A. 2013: Geological and structural model of the Mura–Zala Basin and its rims as a basis for hydrogeological analysis (in Hungarian). *Annual report of the Hungarian Geological Institute 2011*, 47–92.

Fodor L., Héja G., Kövér S., Csillag G. & Csicsek Á. 2017: Cretaceous deformation of the south-eastern Transdanubian Range Unit, and the effect of inherited Triassic–Jurassic normal faults. Pre-conference Excursion Guide. In: *15th Meeting of the Central European Tectonic Studies Group (CETeG)*, 47–76.

Fodor L., Balázs A., Csillag G., Dunkl I., Héja G., Jelen B., Kelemen P., Kövér S., Németh A., Nyíri D., Selmeczi I., Trajanova M., Vrabec M. & Vrabec M. 2021: Crustal exhumation and depocenter migration from the Alpine orogenic margin towards the Pannonian extensional back-arc basin controlled by inheritance. *Global and Planetary Chang*, 201, 103475. https://doi.org/10.1016/j.gloplacha.2021.103475

Fonnesu M., Felletti F., Haughton P.D., Patacci M. & McCaffrey W.D. 2018: Hybrid event bed character and distribution linked to turbidite system sub-environments: The North Apennine Gottero Sandstone (north-west Italy). *Sedimentology* 65, 151–190. https://doi.org/10.1111/sed.12376

Fugelli E.M.G. & Olsen T.R. 2007: Delineating confined slope turbidite systems offshore mid-Norway: The Cretaceous deep-marine Lysing Formation. *AAPG Bulletin* 91, 1577–1601. https://doi.org/10.1306/07090706137

Gelencsér O., Cseresznyés D., Szamosfalvi Á., Breitner D., Kővágó Á., Szabó Cs., Szabó-Krausz Z. & Falus Gy. 2026: Geological potential of hydrogen storage in the Pannonian Basin complex. *Geological Society, London, Special Publications* 555, SP555-2023-198. https://doi.org/10.1144/SP555-2023-198

Groenenberg R.M., Hodgson D.M., Prélat A., Luthi S.M. & Flint S.S. 2010: Flow–deposit interaction in submarine lobes: insights from outcrop observations and realizations of a process-based numerical model. *Journal of Sedimentary Research* 80, 252–267.

Gyetvai G. 1999: *A Somogyi medence feltöltődésének vizsgálata*. MSc Thesis, Department of Geology, Eötvös Loránd University, Budapest, 1–85.

Haughton P.D.W. 2001: Contained turbidites used to track sea bed deformation and basin migration, Sorbas Basin, south-east Spain. *Basin Research* 13, 117–139. https://doi.org/10.1046/j.1365-2117.2001.00143.x

Haughton P., Davis C., McCaffrey W. & Barker S. 2009: Hybrid sediment gravity flow deposits – Classification, origin and significance. *Marine and Petroleum Geology* 26, 1900–1918. https://doi.org/10.1016/j.marpetgeo.2009.02.012

Horváth F., Musitz B., Balázs A., Végh A., Uhrin A., Nádor A., Koroknai B., Pap N., Tóth T. & Wórum G. 2015: Evolution of the Pannonian basin and its geothermal resources. *Geothermics* 53, 328–352. https://doi.org/10.1016/j.geothermics.2014.07.009

Horváth F., Bada G., Szafián P., Tari G., Ádám A. & Cloetingh S. 2006: Formation and deformation of the Pannonian Basin: constraints from observational data. *Geological Society, London, Memoirs* 32, 191–206. https://doi.org/10.1144/GSL.MEM.2006.032.01.11

Juhász E., Budai T., Farkas-Bulla J., Hámor T., Lantos M., Müller P. & Tóth-Makk A. 1994: *A Pannon-medence Neogén üledékeinek vészletes sedimentológiai fácies-elemzése és értékelése*. Report of the IBS Project, Department of Geophysics, Eötvös Loránd University, Budapest.

Juhász Gy. 1992: A pannóniai (sl) formációk térképezése az Alföldön: elterjedés, fácies és üledékes környezet. *Földtani Közlöny* 122, 133–165.

Kneller B. 2003: The influence of flow parameters on turbidite slope channel architecture. *Marine and Petroleum Geology* 20, 901–910. https://doi.org/10.1016/j.marpetgeo.2003.03.001

Kneller B. & Branney M.J. 1995: Sustained high-density turbidity currents and the deposition of thick massive sands. *Sedimentology* 42, 607–616. https://doi.org/10.1111/j.1365-3091.1995.tb00395.x

Kneller B. & McCaffrey W. 1999: Depositional effects of flow nonuniformity and stratification within turbidity currents approaching a bounding slope; deflection, reflection, and facies variation. *Journal of Sedimentary Research* 69, 980–991. https://doi.org/10.2110/jsr.69.980

Kovács Z. & Gyuricza G. 2015: *Mezőcsokonya szénhidrogén koncesszióra javasolt terület komplex érzékenységi és terhelhetőségi vizsgálati jelentése*. MBFH, Budapest.

Liu Q., Kneller B., Fallgatter C., Valdez Buso V. & Milana J.P. 2018: Tabularity of individual turbidite beds controlled by flow efficiency and degree of confinement. *Sedimentology* 65, 2368–2387. https://doi.org/10.1111/sed.12470

Lomas S.A. & Joseph P. 2004: Confined turbidite systems. *Geological Society, London, Special Publications*, 222, 1–7.

Magyar I., Geary D.H. & Müller P. 1999: Paleogeographic evolution of the Late Miocene Lake Pannon in Central Europe. *Palaeogeography, Palaeoclimatology, Palaeoecology* 147, 151–167. https://doi.org/10.1016/S0031-0182(98)00155-2

Magyar I. 2021: Chronostratigraphy of clinothem-filled non-marine basins: Dating the Pannonian Stage. *Global and Planetary Change* 205, 103609. https://doi.org/10.1016/j.gloplacha.2021.103609

Magyar I., Radivojević D., Sztanó O., Synak R., Ujszászi K. & Pócsik M. 2013: Progradation of the paleo-Danube shelf margin across the Pannonian Basin during the Late Miocene and Early Pliocene. *Global and Planetary Change* 103, 168–173. https://doi.org/10.1016/j.gloplacha.2012.06.007

Majercsik Cs. 2009: *Selfperemi deltarendszer progradációjának és tektonikai mozgások általi befolyásoltságának vizsgálata a középzalai térség pannóniai üledéksorában*. MSc Thesis, Department of Geology, Eötvös Loránd University, Budapest, 1–100.

Marini M., Patacci M., Felletti F. & McCaffrey W.D. 2016: Fill to spill stratigraphic evolution of a confined turbidite mini-basin succession, and its likely well bore expression: The Castagnola Fm, NW Italy. *Marine and Petroleum Geology* 69, 94–111. https://doi.org/10.1016/j.marpetgeo.2015.10.014

Mutti E. 1999: An Introduction to the Analysis of Ancient Turbidite Basins from an Outcrop Perspective. *AAPG Continuing Education Course Note*, No. 39, AAPG. https://doi.org/10.1306/CE39687

Nyíri D., Tőkés L., Zadravecz Cs. & Fodor L. 2021: Early post-rift confined turbidite systems in a supra-detachment basin: Implications for the early to middle Miocene basin evolution and hydrocarbon exploration of the Pannonian Basin. *Global and Planetary Change* 203, 103500. https://doi.org/doi.org/10.1016/j.gloplacha.2021.103500

Oluboyo A.P., Gawthorpe R.L., Bakke K. & Hadler-Jacobsen F. 2014: Salt tectonic controls on deep-water turbidite depositional systems: Miocene, southwestern Lower Congo Basin, offshore Angola. *Basin Research* 26, 597–620. https://doi.org/10.1111/bre.12051

Oravecz É., Balázs A., Gerya T., May D.A. & Fodor L. 2024: Competing effects of crustal shortening, thermal inheritance, and surface processes explain subsidence anomalies in inverted rift basins. *Geology* 52, 447–452. https://doi.org/10.1130/G51971.1

Oross R. 2015: *A Dráva-medence szerkezetfejlődése és a kapcsolódó gáz/olajmezők viszonya a Barcs környéki területen*. MSc Thesis, Department of Geology, Eötvös Loránd University.

Patacci M., Haughton P.D.W. & McCaffrey W.D. 2014: Rheological complexity in sediment gravity flows forced to decelerate against a confining slope, Braux, SE France. *Journal of Sedimentary Research* 84, 270–277. https://doi.org/10.2110/jsr.2014.26

Patacci M., Haughton P.D.W. & McCaffrey W.D. 2015: Flow Behavior of Ponded Turbidity Currents. *Journal of Sedimentary Research* 85, 885–902. https://doi.org/10.2110/jsr.2015.59

Patacci M., Marini M., Felletti F., Di Giulio A., Setti M. & McCaffrey W. 2020: Origin of mud in turbidites and hybrid event beds: Insight from ponded mudstone caps of the Castagnola turbidite system (north-west Italy). *Sedimentology* 67, 2625–2644. https://doi.org/10.1111/sed.12713

Pickering K.T. & Hiscott R.N. 1985: Contained (reflected) turbidity currents from the Middle Ordovician Cloridorme Formation, Quebec, Canada: an alternative to the antidune hypothesis. *Sedimentology* 32, 373–394. https://doi.org/10.1111/j.1365-3091.1985.tb00518.x

Pickering K.T., Corregidor J. & Clark J.D. 2015: Architecture and stacking patterns of lower-slope and proximal basin-floor channelised submarine fans, Middle Eocene Ainsa System, Spanish Pyrenees: An integrated outcrop–subsurface study. *Earth-Science Reviews* 144, 47–81. https://doi.org/10.1016/j.earscirev.2014.11.017

Pirmez C., Beaubouef R.T., Friedmann S.J. & Mohrig D.C. 2000: Equilibrium profile and baselevel in submarine channels: examples from Late Pleistocene systems and implications for the architecture of deepwater reservoirs. In: *Global deep-water reservoirs: Gulf Coast Section SEPM Foundation 20th Annual Bob F. Perkins Research Conference*, 782–805. https://doi.org/10.5724/gcs.00.15.0782

Prather B.E., Booth J.R., Steffens G.S. & Craig P.A. 1998: Classification, lithologic calibration, and stratigraphic succession of seismic facies of intraslope basins, deep-water Gulf of Mexico. *AAPG bulletin* 82, 701–728.

Prather B.E., Pirmez C. & Winker C.D. 2012: Stratigraphy of linked intraslope basins: Brazos-Trinity system western Gulf of Mexico. In: Application of the Principles of Seismic Geomorphology to Continental-Slope and Base-of-Slope Systems: Case Studies from Seafloor and Near-Seafloor Analogues. *SEPM, Special Publication* 99, 83–109. https://doi.org/10.2110/pec.12.99.0083

Ruszkiczay-Rüdiger Zs., Balázs A., Csillag G., Drijkoningen G. & Fodor L. 2020: Uplift of the Transdanubian Range, Pannonian Basin: how fast and why? *Global and Planetary Change* 192, 103263. https://doi.org/10.1016/j.gloplacha.2020.103263

Selmeczi I. 2018: Magyarország szénhidrogén-kutatási területei – Dél-Dunántúl – Zala- és Dráva-medence. In: *Szénhidrogének Magyarországon*, 51–78.

Sinclair H.D. & Tomasso M. 2002: Depositional evolution of confined turbidite basins. *Journal of Sedimentary Research* 72, 451–456. https://doi.org/10.1306/111501720451

Skorday E. 2010: *Az Ortaháza-Kilimáni-gerinc és északi előterének szerkezete*. MSc Thesis, Eötvös Loránd University, Budapest.

Smith R.U. 2004: Silled sub-basins to connected tortuous corridors: sediment distribution systems on topographically complex subaqueous slopes. *Geological Society, London, Special Publications* 222, 23–43. https://doi.org/10.1144/GSL.SP.2004.222.01.03

Smith R. & Joseph P. 2004: Onlap stratal architectures in the Grès d'Annot: geometric models and controlling factors. *Geological Society, London, Special Publications* 221, 389–399. https://doi.org/10.1144/GSL.SP.2004.221.01.21

Southern S.J., Patacci M., Felletti F. & McCaffrey W.D. 2015: Influence of flow containment and substrate entrainment upon sandy hybrid event beds containing a co-genetic mud-clast-rich division. *Sedimentary Geology* 321, 105–122. https://doi.org/10.1016/j.sedgeo.2015.03.006

Soutter E.L., Bell D., Cumberpatch Z.A., Ferguson R.A., Spychala Y.T., Kane I.A. & Eggenhuisen J.T. 2021: The Influence of Confining Topography Orientation on Experimental Turbidity Currents and Geological Implications. *Frontiers in Earth Science* 8. https://doi.org/10.3389/feart.2020.540633

Sprague A.R.G., Garfield T.R., Goulding F.J., Beaubouef R.T., Sullivan M.D., Rossen C., Campion K.M., Sickafoose D.K., Abreu V., Schellpeper M.E. & others 2005: Integrated slope channel depositional models: the key to successful prediction of reservoir presence and quality in offshore West Africa. *CIPM, cuarto E-Exitep*, 1e13.

Spychala Y.T., Hodgson D.M., Flint S.S. & Mountney N.P. 2015: Constraining the sedimentology and stratigraphy of submarine intraslope lobe deposits using exhumed examples from the Karoo Basin, South Africa. *Sedimentary Geology* 322, 67–81. https://doi.org/10.1016/j.sedgeo.2015.03.013

Spychala Y.T., Hodgson D.M. & Lee D.R. 2017a: Autogenic controls on hybrid bed distribution in submarine lobe complexes. *Marine and Petroleum Geology* 88, 1078–1093.

Spychala Y.T., Hodgson D.M., Stevenson C.J. & Flint S.S. 2017b: Aggradational lobe fringes: The influence of subtle intrabasinal seabed topography on sediment gravity flow processes and lobe stacking patterns. *Sedimentology* 64, 582–608. https://doi.org/10.1111/sed.12315

Stevenson C.J., Talling P.J., Masson D.G., Sumner E.J., Frenz M. & Wynn R.B. 2014: The spatial and temporal distribution of grain-size breaks in turbidites. *Sedimentology* 61, 1120–1156. https://doi.org/10.1111/sed.12091

Straub K.M. & Pyles D.R. 2012: Quantifying the hierarchical organization of compensation in submarine fans using surface statistics. *Journal of Sedimentary Research* 82, 889–898. https://doi.org/10.2110/jsr.2012.73

Šujan M., Aherwar K., Šarinová K., Vlček T., Chyba A., Hudáčková N., Jamrich M., Kováčová M., AsterTeam & Sztanó O. 2025: Hindering the applicability of the authigenic ^{10}Be/^{9}Be dating by redeposition of mud in hybrid event beds, eastern Danube Basin, Slovakia. *Applied Geochemistry* 179, 106254. https://doi.org/10.1016/j.apgeochem.2024.106254

Sylvester Z., Cantelli A. & Pirmez C. 2015: Stratigraphic evolution of intraslope minibasins: Insights from surface-based model. *AAPG Bulletin* 99, 1099–1129. https://doi.org/10.1306/01081514082

Sztanó O., Magyar I. & Horváth F. 2007: Changes of water depth in the Late Miocene Lake Pannon revisited: the end of an old legend. *Geophysical Research Abstracts* 9, 38897836.

Sztanó O., Magyar I., Szónoky M., Lantos M., Müller P., Lenkey L., Katona L. & Csillag G. 2013a: Tihany Formation in the surroundings of Lake Balaton: type locality, depositional setting and stratigraphy. *Földtani Közlöny* 143, 73–98.

Sztanó O., Szafián P., Magyar I., Horányi A., Bada G., Hughes D.W., Hoyer D.L. & Wallis R.J. 2013b: Aggradation and progradation controlled clinothems and deep-water sand delivery model in the Neogene Lake Pannon, Makó Trough, Pannonian Basin, SE Hungary. *Global and Planetary Change* 103, 149–167. https://doi.org/10.1016/j.gloplacha.2012.05.026

Sztanó O., Kováč M., Magyar I., Šujan M., Fodor L., Uhrin A., Rybár S., Csillag G. & Tőkés L. 2016: Late Miocene sedimentary record of the Danube/Kisalföld Basin: interregional correlation of depositional systems, stratigraphy and structural evolution. *Geologica Carpathica* 67, 525–542. https://doi.org/10.1515/geoca-2016-0033

Sztanó O., Magyar I. & Katona L. 2020: A Pannon-tó és a Balaton. In: *A Balaton kutatása Lóczy Lajos nyomdokán.* Magyarhoni Földtani Társulat, Budapest, 107–125.

Sztanó O., Balázs A., Bartha I.R., Ben Mahrez H., Horányi A., Kovács Á., Šujan M., Tőkés L., Törő B., Vallner F., Varga G. & Magyar I. 2026: Sedimentology, lithostratigraphy, palaeogeography and water level changes in a lacustrine basin: the depositional model of Lake Pannon. *Geological Society, London, Special Publications* 554, SP554-2024-72. https://doi.org/10.1144/SP554-2024-72

Talling P.J., Masson D.G., Sumner E.J. & Malgesini G. 2012: Subaqueous sediment density flows: Depositional processes and deposit types. *Sedimentology* 59, 1937–2003. https://doi.org/10.1111/j.1365-3091.2012.01353.x

Tari G., Dövényi P., Dunkl I., Horváth F., Lenkey L., Stefanescu M., Szafián P. & Tóth T. 1999: Lithospheric structure of the Pannonian basin derived from seismic, gravity and geothermal data. *Geological Society, London, Special Publications* 156, 215–250. https://doi.org/10.1144/GSL.SP.1999.156.01.12

Tari G., Bada G., Boote D.R., Krézsek C., Koroknai B., Kovács G., Lemberkovics V., Sachsenhofer R.F. & Tóth T. 2023: The Pannonian super basin: A brief overview. *AAPG bulletin* 107, 1391–1417. https://doi.org/10.1306/02172322098

Terlaky V., Rocheleau J. & Arnott R.W.C. 2016: Stratal composition and stratigraphic organization of stratal elements in an ancient deep-marine basin-floor succession, Neoproterozoic Windermere Supergroup, British Columbia, Canada. *Sedimentology* 63, 136–175. https://doi.org/10.1111/sed.12222

Tinterri R. & Tagliaferri A. 2015: The syntectonic evolution of foredeep turbidites related to basin segmentation: Facies response to the increase in tectonic confinement (Marnoso-arenacea Formation, Miocene, Northern Apennines, Italy). *Marine and Petroleum Geology* 67, 81–110. https://doi.org/10.1016/j.marpetgeo.2015.04.006

Tőkés L. & Patacci M. 2018: Quantifying tabularity of turbidite beds and its relationship to the inferred degree of basin confinement. *Marine and Petroleum Geology* 97, 659–671. https://doi.org/10.1016/j.marpetgeo.2018.06.012

Tőkés L., Bartha I.R., Silye L., Krézsek Cs. & Sztanó O. 2021: Multiple-scale incision-infill cycles in deep-water channels from the lacustrine Transylvanian Basin, Romania: Auto- or allogenic controls? *Global and Planetary Change* 202, 103511. https://doi.org/10.1016/j.gloplacha.2021.103511

Törő B., Sztanó O. & Fodor L. 2012: Inherited and syndepositional structural control on the evolution of the slope of Lake Pannon, Northern Somogy, Hungary. *Földtani Közlöny* 142, 339–356.

Turcotte D.L. & Huang J. 1995: Fractal Distributions in Geology, Scale Invariance, and Deterministic Chaos. In: Barton C.C. & La Pointe P.R. (eds.): *Fractals in the Earth Sciences.* Springer US, Boston, MA, 1–40. https://doi.org/10.1007/978-1-4899-1397-5_1

Uhrin A. 2011: *Vízszintváltozási ciklusok és kialakulásuk okai a késő-miocén Pannon-tó egyes részmedencéiben*. PhD Thesis, Department of Geology, Eötvös Loránd University, Budapest, 1–127.

Uhrin A. & Sztanó O. 2012: Water-level changes and their effect on deepwater sand accumulation in a lacustrine system: a case study from the Late Miocene of western Pannonian Basin, Hungary. *International Journal of Earth Sciences* 101, 1427–1440. https://doi.org/10.1007/s00531-011-0741-4

Uhrin A., Magyar I. & Sztanó O. 2009: Az aljzatdeformáció hatása a pannóniai üledékképződés menetére a Zalai-medencében. *Földtani közlöny* 139, 273–282.

Ustaszewski K., Kounov A., Schmid S.M., Schaltegger U., Krenn E., Frank W. & Fügenschuh B. 2010: Evolution of the Adria-Europe plate boundary in the northern Dinarides: From continent-continent collision to back-arc extension. *Tectonics* 29. https://doi.org/10.1029/2010TC002668

Van der Merwe W.C., Hodgson D.M., Brunt R.L. & Flint S.S. 2014: Depositional architecture of sand-attached and sand-detached channel-lobe transition zones on an exhumed stepped slope mapped over a 2500 km^2 area. *Geosphere* 10, 1076–1093. https://doi.org/10.1130/GES01035.1

Várkonyi A. 2012: *Észak-Somogy késő-kainozoos deformációjának és üledékképződésének vizsgálata szeizmikus adatok alapján*. MSc Thesis, Department of Geology, Eötvös Loránd University, Budapest, 1–97.

Vlček T., Šarinová K., Kováčová M., Sztanó O. & Šujan M. 2024: Sources and composition of organic matter as a tool for understanding the complex variation in paleoenvironments and the connectivity of an epicontinental basin: The Miocene in the northern Pannonian Basin. *Sedimentary Geology* 470, 106721. https://doi.org/10.1016/j.sedgeo.2024.106721

Weimer P., Slatt R.M., Bouroullec R., Fillon R., Pettingill H., Pranter M. & Tari G. 2006: *Introduction to the Petroleum Geology of Deepwater Settings*. https://doi.org/10.1306/St571314

Wynn R.B., Kenyon N.H., Masson D.G., Stow D.A.V. & Weaver P.P.E. 2002: Characterization and recognition of deep-water channel-lobe transition zones. *AAPG Bulletin* 86, 1441–1462. https://doi.org/10.1306/61EEDCC4-173E-11D7-8645000102C1865D